NGR-52-012-006

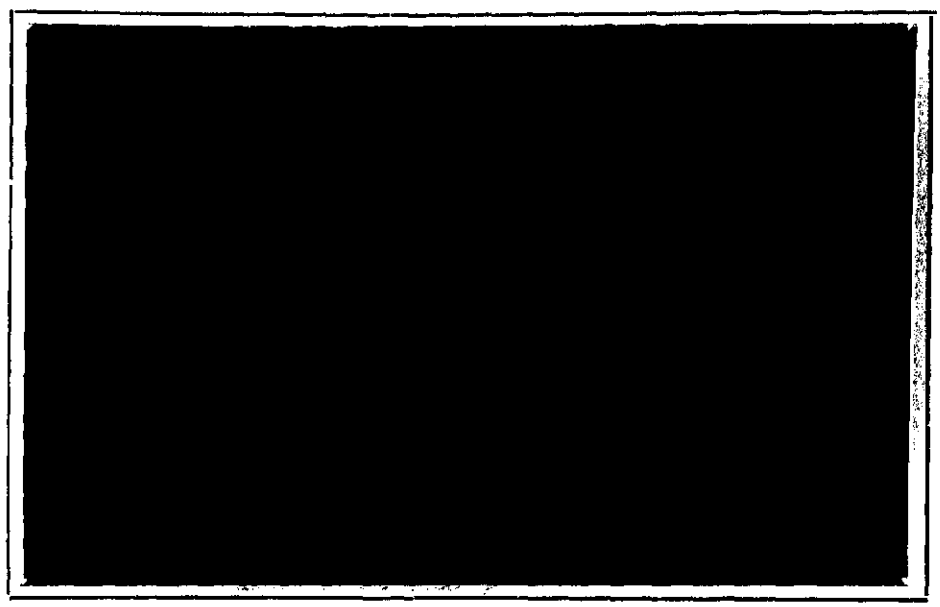

הטכניון – מכון טכנולוגי לישראל
הפקולטה להנדסה אירונוטית

TECHNION — ISRAEL INSTITUTE OF TECHNOLOGY
DEPARTMENT OF AERONAUTICAL ENGINEERING
HAIFA, ISRAEL

(NASA-CR-138658) FLUTTER SUPPRESSION AND GUST ALLEVIATION USING ACTIVE CONTROLS Final Report (Technion - Israel Inst. of Tech.) 83 p HC $7.25 CSCL 01A

N74-26424

G3/01 Unclas 41582

NGR 52-012-006

FINAL REPORT

FLUTTER SUPPRESSION AND GUST ALLEVIATION USING ACTIVE CONTROLS

E. Nissim

Technion - Israel Institute of Technology
Department of Aeronautical Engineering
Haifa, Israel

TAE REPORT No. 198

The research reported in this document has been supported by NASA under Grant NGR 52-012-006.

SUMMARY

The effects of active controls on the suppression of flutter and gust alleviation of two different types of subsonic aircraft (The Arava, twin turboprop STOL transport and the Westwind twin-jet business transport) are investigated. The active controls are introduced in pairs which include,in any chosen wing strip, a leading-edge (L.E.) control and a trailing-edge (T.E.) control. Each control surface is allowed to be driven by a combined linear-rotational sensor system, located on the activated strip. The control law, which translates the sensor signals into control surface rotations, is based on the concept of aerodynamic energy. All but one of the control-law parameters have been pre-optimized using two dimensional aerodynamic theory. The pre-optimized coefficients insure the effectiveness of each of the L.E. - T.E. systems in controlling any type of disturbance. The best locations of a single active system, are determined for the purpose of flutter suppression and for the purpose of gust alleviation (which includes alleviation of the maximum bending moment of the wing and alleviation of the accelerations along the fuselage, including the c.g. of the aircraft). Optimum locations for multi-sets of active controls are also determined.

The results indicate the extreme effectiveness of the active systems in controlling flutter: A single system, for example, spanning 10% of the wing semi-span made the Arava flutter-free (increase in flutter speed could not be determined but is known to be much larger than 70% increase).A similar active

system, for the Westwind aircraft, yielded a reduction of 75% in the maximum bending moment of the wing and a reduction of 90% in the acceleration of the c.g. of the aircraft. Results for simultaneous activation of several L.E. - T.E. systems are presented. Further work needed to bring the investigation to completion is also discussed.

TABLE OF CONTENTS

LIST OF SYMBOLS

b	semichord length
e	distance between mid-chord and leading-edge of control surface (also designated as ℓ_8)
$F(\omega)$	Fourier transform function defined by eqn. (A17)
$F(k)$	real part of the Theodorsen Function
$G(k)$	imaginary part of the Theodorsen Function
$h,\bar{h}$	displacements defined in sketches (A1) and (A2), respectively.
I,I_j	integrals defined by eqns. (A21) and (A24), respectively
J_j	integral defined by eqn. (A25)
k	reduced frequency, $\frac{\omega b}{U}$
$\ell_1,\ell_2,\ell_3,\ell_4,\ell_8$	distances defined in sketch (A2)
L,M,T,P,Q,R	aerodynamic forces defined in sketch (A2)
$L_j,M_j,T_j,P_j,$ Q_j,R_j	constituents of L,M,T,P,Q,R respectively, comprised in $[A_o]$
p	$-\frac{1}{3}(1 - 4b^2)^{3/2}$
q_i	i^{th} generalized coordinate
$Q_{h/b},Q_\alpha,Q_\beta,Q_\delta$	generalized aerodynamic force along h/b, α,β,δ, respectively
s	non-dimensional distance, $\frac{Ut}{b}$
t	time
T_j	j^{th} Theodorsen T function
U	flight speed

$W_{h/b}, W_\alpha, W_\beta, W_\delta$	virtual work along coordinates h/b, α, β, and δ, respectively
α, β, δ	rotations defined in sketch (A1)
$\bar{\alpha}, \bar{\beta}, \bar{\delta}$	rotations defined in sketch (A2)
$\phi(s)$	Wagner function
ϕ	j^{th} Kussner ϕ function
ρ	fluid density
ω	oscillatory frequency
ω_r	reference frequency

Matrices

$[A_o]$	aerodynamic coefficients matrix defined by eqn. (A11b)
$[A_1], [A_2]$	aerodynamic matrices defined by eqns. (A40) and (A41) respectively
$[B_1], [B_2]$	aerodynamic matrices defined by eqns. (A42) and (A43) respectively
[C]	control law matrix defined by eqn. (1)
[D]	transformation matrix, defined by eqn. (A11a)
[E]	aerodynamic matrix defined by eqn. (A44)
[G]	control law matrix defined by eqn. (1)
$[H_o], [H_1]$	matrices of aerodynamic coefficients defined by eqns. (A13) and (A14), respectively.
[R]	control law matrix defined by eqn. (1)

Other notations

$[\ ]^T$	transposed matrix
$\{\ \}$	column matrix

Subscripts

s	step type variation
δ	parameter relates to δ

Dots over symbols denote derivatives with respect to time.

LIST OF FIGURES

FIGURE NO.

23 Variation with time of the maximum wing bending moment (at station 5) due to a step up gust - Arava transport with 3 L.E. - T.E. active systems: two located at stations 2 and 3 and one located at various stations along the wing.

24 Variation of the flutter speed of the Arava transport with the location of a single L.E. - T.E. active system at the various stations along the wing.

LIST OF TABLES

I. INTRODUCTION

The technological advances made in recent years in the field of control systems have stimulated considerable interest towards the evaluation of the advantages gained in incorporating active control systems in aircraft (ref. 1). The potentials of active controls regarding gust alleviation and mode stabilization have been evaluated for some specific aircraft such as the XB-70 (refs. 2,3) and B-52 (refs. 4,5). Within the last few years, control systems that suppress lower frequency structural modes have evolved from analytical feasibility study to production hardware. Such systems, controlling the response of the rigid body mode and one elastic mode (first aft body bending) to gust inputs, had recently been successfully installed on the B-52G and H fleet. It resulted in reduced gust loads and a considerable extension of the fatigue life of the aircraft (ref. 6). Some recently developed hardware indicates that from technological point of view, flutter suppression systems (controlling higher frequency unstable modes) are now feasible. Analytical feasibility studies have shown that in many instances, weight savings by, as much as 4% of the total structure weight of large a/c like the SST or the B-1 can be achieved by suppressing flutter by methods other than the variation of the stiffness. This is a considerable weight saving when considering that the payload may be as small as 20% of the structural weight (refs. 7,8).

NASA-LARC had recently embarked on an experimental flutter suppression program to evaluate some analytically obtained results. Initial results (ref. 9) provide an experimental verification of the possibilities to suppress flutter by active controls.

Vital element in all active control systems relate to the choice of sensors (e.g. linear accelerometers, rotational accelerometers, velocity sensors etc), location of the sensors along the span, choice of control surfaces (such as leading-edge (L.E.) controls, trailing-edge (T.E.) controls or canard surfaces) and the location of those controls. Finally, a control law must be established so as to obtain beneficial results for all the modes to be controlled, and for the different flight configurations. Since the number of free parameters available to the system is large, preliminary assumptions are made by the different investigators through which arbitrary values are assigned to some of the parameters. As a typical example one can mention that the choice of sensors or type of control surface is seldom justified beyond some very general type of reasoning. Furthermore, the control law is often formulated by intuitive reasoning, involving a damping type control force (lags displacement by 90 degrees). There remains therefore, to optimize the remaining parameters such as sensor and control surface locations in addition to some gain parameter in the control law. Optimiztion is then achieved for a specific flight configuration. The behaviour at other configurations is then checked for possible deterioration. When such a deterioation is observed (as it often does) it requires a lot of art to proceed with the optimization. When it is remembered that damping type forces are known to lead to flutter instabilities (refs. 10, 11, 12), one tends to reach the conclusion that too many parameters are assumed a priori, leaving too few for optimization. In an attempt to reach an optimization procedure which does not exhibit sensitivity to flight configuration and to reduce to minimum the number of arbitrarily assumed

parameters, the aerodynamic energy concept was developed (ref. 13, 14). The following general results are obtained using the aerodynamic energy analysis:

a) Optimum systems should include both L.E. and T.E. control surfaces in each controlled strip.

b) Optimum systems should be activated by both linear and rotational sensors, located on the activated strip.

c) Very general control laws can be assumed and the coefficients are determined for optimum performance irrespective of the type of aircraft, mass and stiffness distribution, c.g. or elastic axis locations, reduced frequency or Mach number (within the subsonic range).

The remaining parameters, such as spanwise location of the active strips and some free gain parameters can be determined for specific aircraft together with the magnitude of the improvement obtained.

It is the purpose of the following work to apply these initially optimized results, obtained through the use of the aerodynamic energy method, to specific aircraft.Since these (initially optimized) results are effective for both gust alleviation and mode stabilization (including flutter suppression), optimization of the remaining free parameters is performed bearing all those cases in mind, i.e. optimization is performed for:

a) Maximum flutter speed

b) Minimization of the maximum bending moment on the wing

c) Minimization of the accelerations along the fuselage of the aircraft (including c.g. accelerations).

II. CONTROL LAW

The aerodynamic forces acting on a wing section depend on the displacement h/b of a reference point along the chord(measured in semi-chord lengths b), the angle of rotation α and their first and second time derivatives, i.e. $\dot{h}/b$, $\dot{\alpha}$, $\ddot{h}/b$ $\ddot{\alpha}$. Hence it can be expected that the L.E. rotation β of the control surface and the T.E. control rotation δ will be a function of the above parameters, i.e.

$$\begin{Bmatrix}\beta\\ \delta\end{Bmatrix} = [C] \begin{Bmatrix}h/b\\ \alpha\end{Bmatrix} + \omega_r [G] \begin{Bmatrix}\dot{h}/b\\ \dot{\alpha}\end{Bmatrix} + \frac{1}{\omega_r^2} [R] \begin{Bmatrix}\ddot{h}/b\\ \ddot{\alpha}\end{Bmatrix} \tag{1}$$

where [C], [G] and [R] are square 2 x 2 matrices. The matrix [R] can be neglected since the dependence of the aerodynamic forces on the accelerations is relatively small at the normal range of frequencies. The reference frequency ω_r is introduced to maintain the non-dimensionality of eqn. (1). Hence, the following control law will be used throughout the present work

$$\begin{Bmatrix}\beta\\ \delta\end{Bmatrix} = [C] \begin{Bmatrix}h/b\\ \alpha\end{Bmatrix} + \frac{1}{\omega_r} [G] \begin{Bmatrix}\dot{h}/b\\ \dot{\alpha}\end{Bmatrix} \tag{2}$$

The aerodynamic energy analysis shows that the optimum values of [C] and [G] are independent of the value of ω_r. Furthermore, the smaller ω_r is the more effective the active controls become. Eqn. (2) can be written as

$$\begin{Bmatrix} \beta \\ \delta \end{Bmatrix} = [C] \begin{Bmatrix} h/b \\ \alpha \end{Bmatrix} + i \frac{\omega}{\omega_r} [G] \begin{Bmatrix} h/b \\ \alpha \end{Bmatrix} \tag{3}$$

and for ω_r chosen as the mean value of an assigned range of ω it can be taken to be equal to unity yielding

$$\begin{Bmatrix} \beta \\ \delta \end{Bmatrix} = [C] \begin{Bmatrix} h/b \\ \alpha \end{Bmatrix} + i [G] \begin{Bmatrix} h/b \\ \alpha \end{Bmatrix} \tag{4}$$

Eqns. (2) and (4) yield identical optimum values for [C] and [G] (due to their insensitivity to ω_r). Equation (2) is easily mechanized whereas eqn. (4) presents considerable mechanization difficulties. Furthermore, for gust work based on step function analysis eqn. (4) yields the following results:

$$\begin{Bmatrix} \beta_s \\ \delta_s \end{Bmatrix} = [C] \begin{Bmatrix} h_s/b \\ \alpha_s \end{Bmatrix} + i[G] \begin{Bmatrix} h_s/b \\ \alpha_s \end{Bmatrix} \tag{5}$$

where the subscript s denotes step variation. The i in eqn. (5) is meaningless and this stresses the need for using the control law defined by eqn. (2).

III-METHOD OF APPROACH

In an attempt to achieve savings both in labour and time, it was decided to simultaneously tackle the gust and flutter problems through the use of appropriate gust programs. Flutter speed can be detected from a gust program by following the gust response of the aircraft at speeds exceeding the flutter speed (divergent response). It was therefore decided to develop a gust program which would incorporate both L.E. and T.E. control surface movement. Such a gust program could on one hand be based on step gust functions, like the Wagner's function (and its extension to step control movements) and the Kussner gust penetration function. On the other hand, the response of the aircraft to either harmonic or discrete gusts could be achieved by the use of the Fourier transform method.

It appears that the method based on Fourier transforms is advantageous in as far as aerodynamic coefficients are concerned. Oscillatory coefficients for compressible flow, including control surfaces, are more readily available as compared with equivalent Wagner type functions. This is true for both two dimensional wings and finite span wings. Furthermore, the flutter determinant can be readily extracted from the response expressions. Thus, flutter analysis could follow the normal V-g plots.

The available gust program was based on the classical Wagner and Kussner functions. It was therefore decided to use, as a first step, the existing program with modifications relevant to the introduction of L.E. - T.E. control surface rotations. In parallel, a program based on the method of Fourier transforms is currently under development.

The program used in the present work (and which is based on the Wagner and Kussner functions) treats the whole aircraft as one system. It allows for both rigid body translation of the aircraft,rigid body pitch about the c.g. of the aircraft, time lag between wing and tail in gust encounter, and can cope with up to 10 elastic modes of the free-free aircraft. Approximate compressibility effects are simulated by introducing the Prandtl-Glauert correction. Finite span effects are introduced through the square-root factor which yields the well known wing tip singularity. The program allows the introduction of any number of actively controlled L.E. - T.E. strips along the wing and along the horizontal tail. The derivation of aerodynamic forces arising from a step deflection of either the L.E. or T.E. control surface will be discussed in the following.

IV. CONTROL SURFACE AERODYNAMIC FORCES

The generalized aerodynamic forces acting on an airfoil due to a step type rotation of the L.E. and T.E. control surfaces are developed in detail in Appendix A. They can be written as (eqn. A39)

$$\begin{Bmatrix} Q_{h/b} \\ Q_{\alpha} \end{Bmatrix} = \pi\rho b^2 U^2 \left(\phi(s)[A_1] + [A_2]\right) \begin{Bmatrix} \beta_s \\ \delta_s \end{Bmatrix} + \pi\rho b^3 U \left(\phi(s)[B_1] + [B_2]\right) \begin{Bmatrix} \dot{\beta}_s \\ \dot{\delta}_s \end{Bmatrix} + \pi\rho b^4 [E] \begin{Bmatrix} \ddot{\beta}_s \\ \ddot{\delta}_s \end{Bmatrix} \tag{6}$$

where ρ represents the air density, U the air speed, $\phi(s)$ the Wagner function. The matrices $[A_1]$, $[A_2]$, $[B_1]$, $[B_2]$ and $[E]$ are constant 2×2 matrices defined in eqns. (A40) - (A44). Here again, subscript s denotes step type variation of the parameter, whereas the parameter s is defined as

$$s = \frac{Ut}{b}$$

where t denotes time.

The generalized forces $Q_{h/b}$ and Q_{α} represent, respectively, the generalized lift force and moment (about a reference point) acting on the airfoil.

Substituting the control law, as given by eqn. (2), into eqn. (6) we obtain the following expression for the generalized forces:

$$\begin{Bmatrix} Q_{h/b} \\ Q_{\alpha} \end{Bmatrix}_s = \pi\rho b^2 U^2 [(\phi(s)[A_1] + [A_2])[C]] \begin{Bmatrix} h/b \\ \alpha \end{Bmatrix}_s +$$

$$+ \pi\rho b^2 [\frac{U^2}{\omega_r} (\phi(s)[A_1] + [A_2])[G] + bU(\phi(s)[B_1] + [B_2])[C]] \begin{Bmatrix} \dot{h}/b \\ \dot{\alpha} \end{Bmatrix}_s +$$

$$+ \pi\rho b^3 [\frac{U}{\omega_r} (\phi(s)[B_1] + [B_2])[G] + b[E][C]] \begin{Bmatrix} \ddot{h}/b \\ \dot{\alpha} \end{Bmatrix}_s +$$

$$+ \pi\rho b^4 [\frac{1}{\omega_r} [E][G]] \begin{Bmatrix} \ddot{h}/b \\ \ddot{\alpha} \end{Bmatrix}_s \qquad (7)$$

Eqn. (7) can be readily introduced into any existing gust program which is based on the direct use of the Wagner function.

V. OPTIMIZATION PROCEDURE

The optimization procedure allows the variation of two main parameters:

1) The spanwise location of the activated L.E. - T.E. strip along the wing or horizontal tail.

2) The number of simultaneously active control strips.

Each active strip located along the wing is allowed a span equal to 10% of the wing semi-span. Hence ten stations are allowed along each wing (Fig. 1). Each station can accomodate an active strip. The strips located along the horizontal tail are allowed to have spans equal to 1/3 of the horizontal tail semi-span (for the Aravą aircraft only since no active strips were located on the horizontal tail of the westwind aircraft). All L.E. and T.E. control surfaces are allowed 20% chord.

As already mentioned, the smaller the reference frequency ω_r is, the more effective the active controls become. The limitation on the value of ω_r is determined through the angles of control surface rotation allowed to the system. This can be readily seen from eqn. (2). It is also evident that once the limiting values for β and δ are set, the smallest value of ω_r will depend on both the location of the active strip and the magnitude of the gust disturbance (including the airspeed of the aircraft).

As regards the gust disturbance, it is assigned the maximum value requested by the U.S. licensing authorities. Therefore, the limiting value of ω_r depends only on the spanwise location of the active strip. The following procedure was

adopted for the determination of the minimum value of ω_r : -

1) For a maximum gust disturbance and a specific spanwise location of a single active strip, ω_r is varied.

2) The resulting variation with time of β and δ are examined.

3) A value of ω_r is chosen so that the maximum rotation of the controls does not exceed 16°.

4) The above procedure is repeated for four different spanwise locations along the wing, and the limiting values of ω_r for each of those locations is thus determined.

5) Linear interpolation is then used to determine the limiting values of ω_r for intermediate spanwise locations of the active control strips.

It should be noted that when two control strips are simultaneously activated, smaller values of ω_r may be used in each strip. Such a procedure may be adopted in a detailed design process. However, since the present work is aimed at the gauging of the potentials of such systems, refinements of the above nature have not been introduced.

The second step involves optimization with respect to the spanwise location as parameter. The following procedure has been adopted:

a) A single L.E. - T.E. control strip (with its appropriate value of ω_r) is activated at a single station along the wing or tail and the response of the aircraft to maximum gust excitation is then determined.

b) The above procedure is repeated for all the stations and the response is processed for the three criteria mentioned earlier, i.e.:

   1. Maximum increase in flutter speed,
   2. Minimization of the maximum bending moment on the wing.
   3. Minimization of the accelerations along the fuselage of the aircraft (including c.g. accelerations).

   The optimum spanwise location for each of the above criteria is thus determined.

c) Two simultaneously active strips are then allowed. One active strip is located at the optimum station determined at (b) for the appropriate criterion, whereas the second strip is allowed to be located at any of the remaining stations. The response is then processed as before to determine the optimum location for two active strips.

d) A procedure similar to (c) can be applied, if necessary, to obtain the optimum location of three or more simultaneously activated strips.

VI. OUTPUT OF RESULTS

For any combination of activated control strips, the program provides the following output information as a function of time:

1) Maximum wing bending moment,

2) h/b, α, $\dot{h}/b$, $\dot{\alpha}$, $\ddot{h}/b$, $\ddot{\alpha}$ relevant to three points along the fuselage (one of these points coincides with the c.g. of the aircraft).

3) β and δ of the optimizing strip when it coincides with any of the four predetermined stations along the span.

For flutter runs, the output has been reduced to yield h/b and α as a function of time) at the above four predetermined stations, and at one station on the horizontal tail, irrespective of the location of the optimizing strip.

VII. DESCRIPTION OF THE AIRCRAFT USED FOR OPTIMIZATION

The complete geometric and dynamic data of only two aircraft was made available to the writer for the purpose of the present investigation. These include the twin-boom Arava STOL transport and the Westwind business jet transport. Several applications were made to obtain the data relevant to the B-52 bomber, which was the subject of many previous investigations in the field of active controls. This would have enabled to make comparisons between results obtained through the use of the aerodynamic energy concept with those obtained through the use of other methods and which appear in the literature. Such comparisons could reveal the relative power of the energy method. However, in the absence of data relevant to the B-52 bomber, all investigations reported herein have been limited to the aircraft mentioned above.

The Arava aircraft (Fig. 2)

The Arava is a light STOL twin-turboprop transport (max weight 15,000 lb). The high wings are hinged (in bending) at their roots and retained by struts, which are attached to the wing at points lying ahead of the quarter chord point. The twin boom structure which carries the tail unit provides strong elastic coupling between wing and tail. In general the aircraft is highly elastic and is not representative of light transport.

The Westwind aircraft (Figure 3)

The Westwind is the IAI improved version of the Rockwell Jet Commander. It is a twin-jet business transport with a cantilevered wing (max. weight 20,700 lb). The wing is clean with engines fitted at the rear of the fuselage and carries empty tip tanks (chosen configurations). From an aeroelastic point of view, the Westwind aircraft is conventionally built, and therefore, the results are more representative for its class than the Arava.

VIII. PRESENTATION AND DISCUSSION OF RESULTS

The results are presented and discussed in three groups. These groups relate to the effect of active controls on the maximum bending moment at the wing, the fuselage accelerations, and the flutter speed. Each such group contains the results available for both the Arava and the Westwind transports and is accompanied by a discussion of these results. Mention should be made here that the results relating to the Westwind aircraft are of partial nature only and have not been brought to completion. The results relating to the Arava are extensive but also incomplete since little work has been done regarding active controls on the horizontal tail.

The results of the Arava transport are appropriate for a flight speed of 95 m/sec (except for flutter) and step up gust of 10 m/sec. Similarly, the Westwind results relate to a flight speed of 253 m/sec and a step up gust of 15 m/sec.

a) Effect of Active Controls on the Fuselage Accelerations

Three points were chosen to indicate the accellerations of the fuselage due to the step gusts. One of these points coincides with the C.G. of each of the aircraft. A second point, designated as Point 1, is located along the axis of the fuselage, aft of the C.G., and a third point, designated as Point 2 is located along the same axis, fore of the C.G.. For the Arava

transport, Points 1 and 2 are located at 3 meters aft and 3 meters fore of the C.G.. For the Westwind transport, Points 1 and 2 are located at 6.17 meters aft and 6.83 meters fore of the C.G.. Considering the fact that both of the aircraft under investigation are transport planes, a reduction in the accelerations at the above 3 points, which span the length of the fuselage, has a strong influence on the ride comfort of the aircraft. A special importance is attached to the reduction in the accelerations at the C.G. of the aircraft. This is true since no systematic attempts were made to control either the rigid body pitch or the fuselage bending of the aircraft through appropriate activation at the horizontal tail. Therefore, the effectiveness of the active systems located along the wings as regards accelerations, should be measured by the reductions achieved at the C.G., whereas the deviations from the C.G. at Points 1 and 2 indicate the potential benefits obtained through the activation of the horizontal tail (a discussion regarding the interrelations between pitch control and C.G. accelerations is made later in this section).

It has already been mentioned that the smaller the reference frequency ω_r is the more effective the active control becomes. This is shown in general terms in ref. 13. Fig. 4 shows the effect variation of ω_r on the C.G. acceleration of the Arava for a single active system located at station 10 (at the root of the wing). These results are in conformity with the above statement concerning the effect of ω_r. Minimum values of ω_r, for each station, were limited to insure reasonable maximum control surface rotations. It is found that the main constraints come about due to the relatively large rotations of the L.E. controls. These

rotations increase as ω_r decreases. Minimum values of ω_r which maintain the values of β to levels below 16° at the above stated flight speeds and up-gust disturbances, are listed in Table I for the Arava and in Table II for the Westwind. All of the results reported herein are based on the above minimum values of ω_r.

The effect on the C.G. acceleration of the Arava of a single L.E. - T.E. system located at the various stations along the wing is shown in Fig. 5. Similar effects of a single system on the C.G. acceleration of the Westwind is shown in Fig. 6. The results of both aircraft show that the effectiveness of a single L.E. - T.E. system increases steadily as the location of the system moves from the wing tip towards the root of the wing. The maximum effectivenss is obtained at station 10 (which is located at the wing root). The maximum reduction in C.G. accelerations due to a single active system can be seen to amount to 22% for the Arava and to 90% for the Westwind. The effect of introducing a second active system for the Arava in addition to the one at station 10 is shown in Fig. 7. Here again one sees that the best location for the second system is near the root of the wing which means in this case, at station 9. The combined effect of the two systems can be seen to bring about a reduction of 31% in the peak acceleration although larger reductions in acceleration levels can be observed beyond the first peak. No simultaneous activation beyond a single system had so far been attempted for the Westwind. Figure 7 shows the results obtained by activating 3 systems along the wing, keeping two active systems fixed at stations 9 and 10. As expected, best results are obtained when the third active system is

nearest to the root, i.e. at station 8. The reduction in C.G. acceleration due to the three active systems is thus brought to 37%. It can be noted here, once again, that the effect of the three systems beyond the first peak is very large. In an attempt to get some understanding into the behaviour of the first peak, a single run was made with ten active systems spanning the whole of the wing semi-span. The result is shown in Fig. 8. It can be seen that the reduction achieved in the level of the C.G. acceleration amounts to 55% whereas the accelerations beyond this peak are almost negligible. It is interesting to note that the first peak is obtained just before the gust front hits the horizontal trail. It could be expected that during this short interval, when only the wing senses the step up gust, the lift forces which build-up will be destabilizing and will lead to a pitch-up which, in turn, increases the C.G. acceleration. Therefore, a reduction in the lift force build-up through the introduction of the active systems can be expected to be stabilizing and bring about a reduction in the pitch-up which in turn reduces the C.G. acceleration. This, however is not the case as illustrated in Fig. 9, which shows the variation with time of the C.G. angular acceleration of the Arava with three active systems located at stations 8,9 and 10. It can be seen that the contrary is achieved since the introduction of the 3 active systems lead to an increase in pitch-up. To understand this phenomenon it should be remembered that the twin-boom tail unit of the Arava is very flexible and is attached to the wings at around their quarter semi-span points. Therefore, a large acceleration at the C.G. due to a sudden lift build-up at the wings causes large down delfection of the

booms due to inertia effects which, in turn, means an increase in the angle of attack of the horizontal tail. This increase in the angle of attack of the horizontal tail leads to stabilizing forces which bring about a pitch down of the aircraft. Hence, a decrease in the C.G. acceleration due to the introduction of the active systems reduces the inertia effects on the tail and thus reduces stability at the onset of the motion. Once the gust hits the horizontal tail stability is increased again and a rapid oscillatory decay in C.G. accelerations follows. The structure of the aft of the fuselage of the Westwind is much stiffer than the Arava twin boom tail unit and therefore, the fuselage bending due to the above mentioned inertia effects are expected to be very small. Figure 10 which describes the variation with time of the C.G. angular acceleration of the Westwind for a single active system at station 10, supports the above argumentation.

The results regarding the linear accelerations at Point 1 are summarized in Fig. 11, 12, 13 for the Arava and in Fig. 14 for the Westwind. Similar results relating to Point 2 are summarized in Figs. 15, 16, 17 and in Fig. 18 for the Arava and Westwind, respectively. Comparisons between the accelerations at Points 1 and 2 due to a single active system (Figs. 11, 15) acting on the Arava clearly show the above mentioned initial pitch-up and its increase as the active system is moved towards the root of the wing. The increased effectiveness in reducing the accelerations following the first peak can clearly

be seen. Similar comparisons made between Points 1 and 2 for a single active system(Figs. 14, 18) acting on the wings of the Westwind shows that the active system introduces stabilizing effects and thus reduces the initial pitch-up. These stabilizing effects increase as the active system moves towards the root of the wing. However, once the upgust hits the tail, a strong pitch down follows which results in an almost unaffected negative peak value of the acceleration at point 2 (although the positive acceleration is greatly reduced).

As already stated, simultaneous activation of two and three system were introduced only for the case of the Arava transport. The results regarding the linear accelerations at Points 1 and 2 with multi-active system are shown in Figs. 12, 13, 16, 17 and the persistence of the initial peak is very clearly illustrated in Fig. 17. The variation follows the same pattern as the one observed for the single system but with increased effectiveness, especially after the first peak.

On the basis of the results obtained so far, it can be concluded that for very flexible aircraft, such as the Arava, pitch control is necessary in addition to the direct wing lift control in order to efficiently reduce the C.G. accelerations. In stiffer aircraft such as the Westwind, direct lift control on the wing through the introduction of active systems is extremely effective. This effectiveness arises due to the relatively small initial pitch-up. However, pitch control is required for the Westwind to avoid the strong pitch down once the gust front hits the

horizontal tail. Such a control will bring about a uniform reduction of accelerations along the fuselage. It can thus be seen that the potentials of pitch control go beyond the differences between Points 1 and 2.

The simple minded introduction of active L.E. - T.E. systems on the horizontal tail may bring about a further deterioration in stability since the up-acceleration sensed on the tail will activate the controls in such a way as to reduce the lift on the horizontal tail and thus lead to the reduced stability. This statement does not imply that pitch control should be achieved by other active systems. It rather means that the introduction of the L.E. - T.E. systems to the horizontal-tail should be made with care and that some additional sophisticaton needs to be introduced. Very promising ideas to this effect have been suggested and should be tested at a future stage.

In summary it is very important to notice that extremely large reductions in acceleration can be achieved by the introduction of a single active system at the root of the wing. The 90% reduction in C.G. acceleration obtained in the case of the Westwind indicates the potentials of the active systems. With proper pitch control similar very large reductions can be obtained all along the fuselage (large reductions were obtained in the Westwind even in the absence of pitch control), for both the Arava and the Westwind transports.

b) The Effect of Active Controls on the Maximum Wing Bending-Moment

The maximum wing bending moment for the Arava transport is located at the inboard part of station 5 where the struts join the wing. This location is unusual for conventionally built aircraft which have cantilevered wings and therefore develop maximum bending moments at the root of their wings. Such is the case for the Westwind which shows maximum values of bending moment (B.M.) at station 10. Therefore, it should be understood that the results presented herein refer to the B.M.'s at station 5 for the Arava and to the B.M.'s at station 10 for the Westwind.

The effects of a single L.E. - T.E. system, in its various locations along the wing, on the maximum B.M. of the Arava and Westwind transports are shown in Figs. 19, 20, respectively. The best location of the active system on the Arava can be seen (Fig. 19) to be at station 2 (near the tip of the wing). The positive B.M. is reduced by 39% whereas the negative B.M. is greatly increased (in absolute values). For a minimum absolute value of the B.M. the optimum location is at station 3 which yields a reduction of 21% in maximum B.M. Somewhat similar results are shown in Fig. 20 for the Westwind. Here the maximum reduction in the positive B.M. takes place further inboard of the wing, at station 7. It should be observed that the peak positive and negative B.M. are almost equal, leading to a reduction of 77% in the maximum positive B.M. and a reduction of 75% in the B.M. based on absolute peak.

It is interesting to note that an active strip at the tip of the wing is effective in reducing the positive B.M. but at the same time leads to an increase in the negative values of the B.M. This is so since the overall B.M. is an integrated result of the positive moments due to the lift build up as a result of the gust encounter, and the negative moments due to the inertia effects (negative product of the mass acceleration). Since an active strip leads to a reduction of the lift at the station where it is located, it leads to a reduction in the positive moments which means an increase in the negative B.M. This effect could be counteracted if a reduction in the lift force results in a substantial reduction in the accelerations which, in turn, leads to a reduction in the negative B.M.'s.At around the tip of the wing, the lift forces are small and have small effects on the accelerations (but larger effects on the lift moments) giving an overall effect dictated through the reduction of the lift forces, mentioned above. As the active strip moves inboard, the lift force effects of the active strip increase. However, since the distance from the wing root decreases, the resultant overall contribution to the maximum B.M. decreases as the strip moves inboard. As already stated the effect of the active strip on the accelerations of the aircraft increases markedly as the active strip moves inboard. This reduction in the acceleration levels of the wing leads to an increase in the B.M. This is the reason why mid-span locations are found to be most effective in reducing the absolute values of the B.M. Similar results can be obtained by the simultaneous activation of two strips: one location near the wing root (for minimization of the negative B.M.'s) and one located near the wing tip (for minimization

of the positive B.M.'s). Figure 21 shows the effect of introducing a second active system at the various stations along the wing, keeping one active system fixed at station 10. The results show that the best combination is that obtained by placing the second system at station 2. The combined effect reduced the absolute value of the B.M. (A.V.B.M.) by 35%. Since no negative values of B.M. are observed in Fig. 21, some further reduction can be obtained by combining an active system in station 2 with another system at a station outboard of station 10. This is shown in Fig. 22. Stations 6 and 2 give the best combination and yield a reduction of 38% in the A.V.B.M. Fig. 23 shows that the optimum location for 3 systems placed on the wing of the Arava. The best locations for the three systems can be seen to lie at stations 2, 3, and 6 yielding a reduction in the A.V.B.M. of 52%.

The difference between the high effectiveness of a single system on the Westwind as compared with a similar system on the Arava clearly lies in the lack of pitch control discussed earlier. This is true since increased accelerations mean increased aerodynamic loads and thus lead to increased B.M.'s. It is promising however, to realize the effectiveness achieved by a single active system on the Westwind. This effectiveness indicates the potentials to be gained by controlling the pitch angle of the Arava.

Improved results could have been obtained had a filter been used to eliminate the low frequency inputs. This might have led to the elimination

of the large negative values of the B.M. since they exhibit a low frequency variation. It has, however, been preferred to avoid reaching definite conclusions before testing the idea and optimization was performed disregarding the filtering possibility.

In summary it can be stated that the best location of a single active strip regarding the reduction in A.V.B.M. is near the inboard part of the mid-span of the wing. When more than one active system is used, the locations are divided such that some systems lie near the root and some lie near the tip (for B.M. purposes, the Arava span may be considered to extend between stations 1 and 5).

c) The Effect of Active Controls on the Flutter Speed

The effect of active controls on the flutter speed has, so far, been tested on the Arava only. The effect of active controls on the Westwind will be tested in the future.

The results relating to the effect of a single L.E. - T.E. system located at the various stations along the wing are shown in Fig. 24. It can be seen that for a system located at station 1-6, no flutter could be detected even at speeds as high as 70% beyond the reference flutter speed (i.e. flutter speed with no active controls). No attempt was made to go beyond the 70% increase in speed since the aircraft was already in the supersonic regime,

flying on subsonic aerodynamics... Remebering that the flutter speed of the Arava in the configuration considered here is 233 m/sec, an increase of 70% in the flutter speed brings the flight speed to around 400 m/sec. Clearly, there is no point in pushing up the flight speed even for the purposes of rough indications. The trends, however show, that best location for an active system on the Arava is around the outboard part of the wing.

IX. CONCLUDING REMARKS

The effectiveness of activated L.E. - T.E. control systems in gust alleviation and flutter suppression has been demonstrated in the present work. It is remarkable to observe that a "utility" type, preoptimized control law which is based on the concept of aerodynamic energy, brings about such stable and powerful active control systems.

The optimum locations of the active L.E. - T.E. systems for alleviating either fuselage accelerations or maximum B.M. and for suppressing flutter have been determined. The locations of the active systems for the simultaneous alleviation of the above two gust effects together with the suppression of flutter can be readily determined. It is envisaged that two active systems will be required on the wing: one near the root of the wing and the other near the tip. The active system near the root of the wing will mainly reduce the fuselage accelerations whereas the system near the tip of the wing will mainly suppress flutter. The combination of these two systems will be effective to reduce the maximum A.V.B.M. A pitch-control through an active system shows promise in increasing the effectiveness of the active systems located on the wing. It can thus be seen that some insight has been gained regarding the introduction of active controls in the two aircraft under investigation. Much still needs to be done to bring this work to a reasonable completion. Some of the main points are listed below:

a) Completion of the Arava and Westwind investigation

   1) Completing the investigation of the Westwind

   2) Developing and analytically testing an appropriate pitch control based on the concept of aerodynamic energy.

   3) Studying the effects of real systems through the introduction of some phase lags and wash-out filters.

b) Carrying similar investigation on other types of aircraft such as a bomber, a fighter and a large transport etc., using the above results as guidelines.

c) Expanding the aerodynamic energy concept into the supersonic regime.

d) Introducing refinements through improvements made in the aerodynamic theories (such as accurate compressibility corrections, lifting surface theories, etc.).

It is believed that the initial results obtained in the present work warrant the extensiveness of the investigations outlined above.

APPENDIX A

Derivation of the Generalized Aerodynamic Forces of a L.E. - T.E. System Due to a Unit Step Rotation of the Control Surfaces

Let us first consider the determination of the aerodynamic oscillatory forces acting on the system shown in sketch (A1).

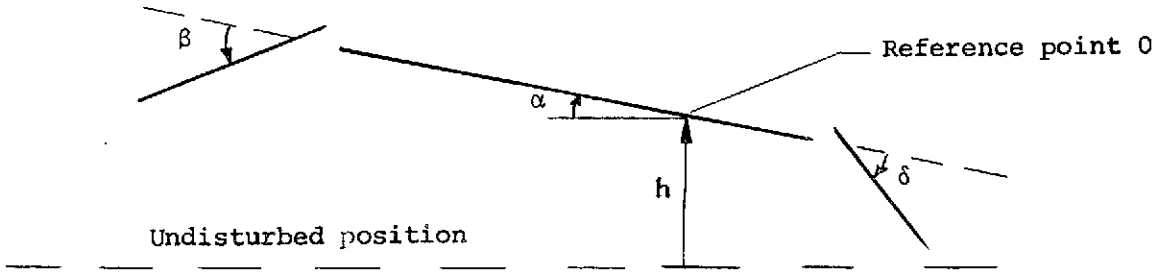

Sketch (A1)

and assume that the oscillatory forces acting on a somewhat similar system (as used in refs. 15, 16) described in sketch (A2) are known. Note the difference between the h, α, β, δ coordinates and the $\bar{h}$, $\bar{\alpha}$, $\bar{\beta}$, $\bar{\delta}$ coordinates. The arrows indicate in each sketch the direction of either positive displacements, forces, or distances.

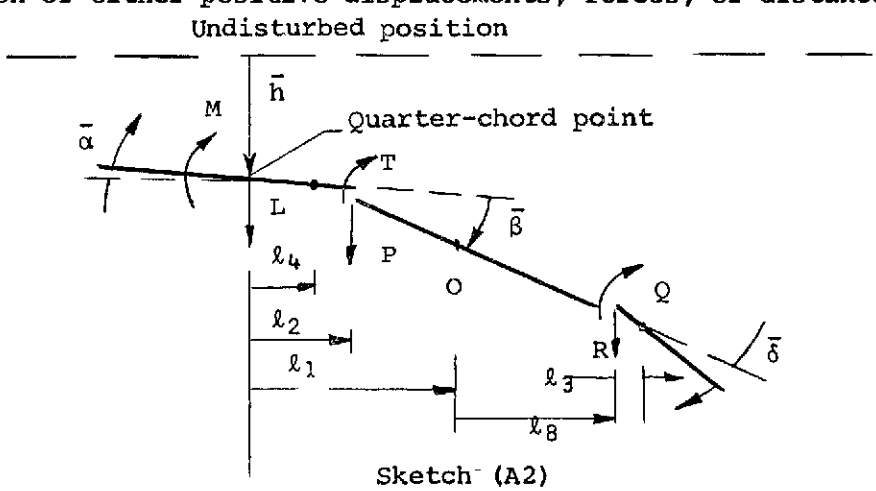

Sketch (A2)

The symbols L and M denote, respectively, the total lift and pitching moment and L is assumed to act through the quarter chord point. The force acting on the aileron-tab combination through the L.E. point is denoted by P and the aileron tab moment is denoted by T. The force acting on the tab moment is Q. The forces in sketch (A2), their direction and points of application are identical with those of Smilg, Wasserman and el. (refs. 15, 16).

As a first stage of the following analysis, the oscialltory generalized forces acting along h, α, β, δ coordinates will be determined through the application of the principle of virtual work.

The virtual work W_h in the h coordinate is given by

$$W_h = - b \frac{h}{b} L \tag{A1}$$

where b represents the semi-chord length. Denoting the generalized forces by subscripted Q's we obtain from eqn. (A1).

$$Q_{h/b} = \frac{\delta W_h}{\delta (h/b)} = - b L \tag{A2a}$$

Similarly, the virtual work W_α in the α coordinate is given by

$$W_\alpha = M \alpha - L \ell_1 \alpha$$

or

$$Q_\alpha = \frac{\delta W}{\delta \alpha} = M - L \ell_1 \tag{A2b}$$

The virtual work W_β in the β coordinate is given by

$$W_\beta = -(M - T - P\ell_2)\beta + (L - P)\ell_4\beta$$

and hence

$$Q_\beta = \frac{\delta W_\beta}{\delta \beta} = P(\ell_2 - \ell_4) + L\ell_4 + T - M \quad . \quad . \qquad \text{(A3)}$$

Similarly

$$W_\delta = Q\delta - R\ell_3\delta$$

or

$$Q_\delta = \frac{\delta W_\delta}{\delta \delta} = Q - R\ell_3 \quad . \quad . \quad . \qquad \text{(A4)}$$

These equations can be condensed into the following matrix eqn.

$$\begin{Bmatrix} Q_{h/b} \\ Q_\alpha \\ Q_\beta \\ Q_\delta \end{Bmatrix} = \begin{bmatrix} -b & 0 & 0 & 0 & 0 & 0 \\ -\ell_1 & 1 & 0 & 0 & 0 & 0 \\ \ell_4 & -1 & 1 & (\ell_2-\ell_4) & 0 & 0 \\ 0 & 0 & 0 & 0 & 1 & -\ell_3 \end{bmatrix} \begin{Bmatrix} L \\ M \\ T \\ P \\ Q \\ R \end{Bmatrix} \qquad \text{(A5)}$$

but the forces are of the form

$$\begin{Bmatrix} L \\ M \\ T \\ P \\ Q \\ R \end{Bmatrix} = \pi\rho\omega^2 \begin{bmatrix} b^3 & & & & & \\ & b^4 & & & & \\ & & b^4 & & & \\ & & & b^3 & & \\ & & & & b^4 & \\ & & & & & b^3 \end{bmatrix} [A_o] \begin{Bmatrix} \bar{h}/b \\ \bar{\alpha} \\ \bar{\beta} \\ \bar{z}/b \\ \bar{\delta} \\ \bar{y}/b \end{Bmatrix} \qquad \text{(A6)}$$

where $[A_o]$ is a 6 x 6 matrix and $\bar{z}$ and $\bar{y}$ define the hinge locations and are given by

$$\bar{z} = (\ell_2 - \ell_4)\bar{\beta}$$

$$\bar{y} = -\ell_3\bar{\delta}$$

Therefore, one can write the following equation based on the latter two eqns.

$$\begin{Bmatrix} \bar{h}/b \\ \bar{\alpha} \\ \bar{\beta} \\ \bar{z}/b \\ \bar{\delta} \\ \bar{y}/b \end{Bmatrix} = \begin{bmatrix} 1 & 0 & 0 & 0 \\ 0 & 1 & 0 & 0 \\ 0 & 0 & 1 & 0 \\ 0 & 0 & \frac{\ell_2-\ell_4}{b} & 0 \\ 0 & 0 & 0 & 1 \\ 0 & 0 & 0 & \frac{-\ell_3}{b} \end{bmatrix} \begin{Bmatrix} \bar{h}/b \\ \bar{\alpha} \\ \bar{\beta} \\ \bar{\delta} \end{Bmatrix} \qquad \text{(A7)}$$

Comparison between the coordinates h, α, β, δ and $\bar{h}$, $\bar{\alpha}$, $\bar{\beta}$, $\bar{\delta}$ yields the following relations: -

$$\bar{h} = (h + \ell_1\alpha - \ell_4\beta)$$

$$\bar{\alpha} = \alpha - \beta$$

$$\bar{\beta} = \beta$$

$$\bar{\delta} = \delta$$

These expressions reduce to

$$\begin{Bmatrix} \bar{h}/b \\ \bar{\alpha} \\ \bar{\beta} \\ \bar{\delta} \end{Bmatrix} = \begin{bmatrix} -1 & -\ell_1/b & \ell_4/b & 0 \\ 0 & 1 & -1 & 0 \\ 0 & 0 & 1 & 0 \\ 0 & 0 & 0 & 1 \end{bmatrix} \begin{Bmatrix} h/b \\ \alpha \\ \beta \\ \delta \end{Bmatrix} \tag{A8}$$

Substitution of eqn. (A8) into eqn. (A7) yields

$$\begin{Bmatrix} \bar{h}/b \\ \bar{\alpha} \\ \bar{\beta} \\ \bar{z}/b \\ \bar{\delta} \\ \bar{y}/b \end{Bmatrix} = \begin{bmatrix} -1 & -\frac{\ell_1}{b} & \frac{\ell_4}{b} & 0 \\ 0 & 1 & -1 & 0 \\ 0 & 0 & 1 & 0 \\ 0 & 0 & \frac{(\ell_2-\ell_4)}{b} & 0 \\ 0 & 0 & 0 & 1 \\ 0 & 0 & 0 & -\ell_3/b \end{bmatrix} \begin{Bmatrix} h/b \\ \alpha \\ \beta \\ \delta \end{Bmatrix} \tag{A9}$$

Substituting eqns. (A6), (A9) into eqn. (A5) we obtain

$$\begin{Bmatrix} Q_{h/b} \\ Q_{\alpha} \\ Q_{\beta} \\ Q_{\delta} \end{Bmatrix} = \pi\rho\omega^2 b^4 \, [D]^T [A_o] [D] \begin{Bmatrix} h/b \\ \alpha \\ \beta \\ \delta \end{Bmatrix} \tag{A10}$$

where

$$[D] = \begin{bmatrix} -1 & -\frac{\ell_1}{b} & \frac{\ell_4}{b} & 0 \\ 0 & 1 & -1 & 0 \\ 0 & 0 & 1 & 0 \\ 0 & 0 & \frac{\ell_2-\ell_4}{b} & 0 \\ 0 & 0 & 0 & 1 \\ 0 & 0 & 0 & -\frac{\ell_3}{b} \end{bmatrix} \qquad \text{(A11a)}$$

Letting

$$[A_o] = \begin{bmatrix} L_1 & L_2 & L_3 & L_4 & L_5 & L_6 \\ M_1 & M_2 & M_3 & M_4 & M_5 & M_6 \\ T_1 & T_2 & T_3 & T_4 & T_5 & T_6 \\ P_1 & P_2 & P_3 & P_4 & P_5 & P_6 \\ Q_1 & Q_2 & Q_3 & Q_4 & Q_5 & Q_6 \\ R_1 & R_2 & R_3 & R_4 & R_5 & R_6 \end{bmatrix} \qquad \text{(A11b)}$$

and using eqn. (A10) we can write

$$\begin{Bmatrix} Q_{h/b} \\ Q_\alpha \end{Bmatrix} = \pi\rho\omega^2 b^4 \left([H_o] \begin{Bmatrix} h/b \\ \alpha \end{Bmatrix} + [H_1] \begin{Bmatrix} \beta \\ \delta \end{Bmatrix} \right) \qquad \text{(A12)}$$

where

$$[H_o] = \begin{bmatrix} [L_1] & [L_1 \frac{\ell_1}{b} - L_2] \\ [L_1 \frac{\ell_1}{b} - M_1] & [\frac{\ell_1}{b}(L_1 \frac{\ell_1}{b} - L_2) - M_1 \frac{\ell_1}{b} + M_2] \end{bmatrix} \quad \text{(A13)}$$

and

$$[H_1] = \begin{bmatrix} H_1(1,1) & H_1(1,2) \\ H_1(2,1) & H_1(2,2) \end{bmatrix}$$

where

$$H_1(1,1) = -\left(L_1 \frac{\ell_4}{b} - L_2 + L_3 + L_4 \frac{(\ell_2 - \ell_4)}{b}\right)$$

$$H_1(1,2) = -L_5 + L_6 \frac{\ell_3}{b}$$

$$H_1(2,1) = M_1 \frac{\ell_4}{b} - M_2 + M_3 + M_4 \frac{(\ell_2 - \ell_4)}{b} - \frac{\ell_1}{b}\left(L_1 \frac{\ell_4}{b} - L_2 + L_3 + L_4 \frac{(\ell_2 - \ell_4)}{b}\right)$$

$$H_1(2,2) = M_5 - M_6 \frac{\ell_3}{b} - \frac{\ell_1}{b}\left(L_5 - L_6 \frac{\ell_3}{b}\right) \quad \text{(A14)}$$

Eqn. (A14) can be written as

$$[H_1] = [T_A][A][T_p] \quad \text{(A15)}$$

where

$$[T_A] = \begin{bmatrix} 1 & 0 \\ \frac{\ell_1}{b} & -1 \end{bmatrix}$$

$$[T_p] = \begin{bmatrix} -\frac{\ell_4}{b} & 0 \\ 1 & 0 \\ -1 & 0 \\ \frac{(\ell_2 - \ell_4)}{b} & 0 \\ 0 & -1 \\ 0 & \ell_3/b \end{bmatrix}$$

and

$$[A] = \begin{bmatrix} L_1 & L_2 & L_3 & L_4 & L_5 & L_6 \\ M_1 & M_2 & M_3 & M_4 & M_5 & M_6 \end{bmatrix}$$

In order to compute the forces due to control surface step rotations, use of Fourier Integrals will be made to superimpose the various sinusoidal forces into the necessary force, i.e.,

$$q_i(t) = \frac{1}{2\pi} \int_{-\infty}^{\infty} F(\omega) e^{i\omega t} \, d\omega \tag{A16}$$

$$F(\omega) = \int_{-\infty}^{\infty} q_i(t) e^{-i\omega t} \, dt \tag{A17}$$

where $q_i(t)$ is the generalized i^{th} coordinate. For a q_i step function of amplitude q_{is}, eqn. (A17) yields a frequency spectrum of

$$F(\omega) = \frac{q_{is}}{i\omega} \tag{A18}$$

with amplitudes, as given by eqn. (A16), i.e.,

$$dq_i = \frac{1}{2\pi} F(\omega) e^{i\omega t} \, d\omega$$

or

$$dq_i = \frac{q_{is}}{2\pi} \frac{e^{i\omega t}}{i\omega} \, d\omega \tag{A19}$$

Equation (A12) yields the aerodynamic forces for any frequency. Hence substituting eqn. (A19) into eqn. (A12) and integrating over the whole spectrum which constitutes a step variation in amplitude, we obtain

$$\left\{\begin{matrix} Q_{h/b} \\ Q_{\alpha} \end{matrix}\right\}_s = \pi\rho b^4 \int_{-\infty}^{\infty} \frac{\omega^2 e^{i\omega t}}{2\pi i\omega} \left([H_o] \left\{\begin{matrix} h_{s/b} \\ \alpha_s \end{matrix}\right\} + [H_1] \left\{\begin{matrix} \beta_s \\ \alpha_s \end{matrix}\right\} \right) d\omega \qquad \text{(A20)}$$

where the subscript s refers to step variation. Eqn. (A20) requires the evaluation of integrals of the type

$$\left.\begin{aligned} I &= q_{rs} \int_{-\infty}^{\infty} L_j \frac{\omega^2 e^{i\omega t}}{2\pi i\omega} \, d\omega \\ \text{or} \qquad I &= q_{rs} \int_{-\infty}^{\infty} M_j \frac{\omega^2 e^{i\omega t}}{2\pi i\omega} \, d\omega \end{aligned}\right\} \qquad \text{(A21)}$$

The functions L_j and M_j can be represented in their most general form by the following quadratic expression in $\frac{1}{k}$ (illustrated for L_j): -

$$L_j = [a_o + (F + iG)d_o] + [a_1 + (F + iG)d_1]\frac{1}{k} + [a_2 + (F + iG)d_2]\frac{1}{k^2} \qquad \text{(A22)}$$

where the a_j's and d_j's are constants and $(F + iG)$ represents the Theodersen Function which varies with k. Hence, the evaluation of eqn. (A21) requires the evaluation of the following basic integrals

$$\left.\begin{aligned} I_j &= q_{rs} a_j \int_{-\infty}^{\infty} \frac{\omega^2 e^{i\omega t} d\omega}{2\pi i\omega (k)^j} \\ J_j &= q_{rs} d_j \int_{-\infty}^{\infty} \frac{(F + iG)\omega^2 e^{i\omega t} d\omega}{2\pi i\omega (k)^j} \end{aligned}\right\} \qquad \text{(A23)}$$

Remembering that

$$\omega = \frac{U}{b} k$$

and letting

$$s = \frac{Ut}{b}$$

which leads to

$$\omega t = ks$$

we can write

$$I_j = q_{rs} a_j \frac{U^2}{b^2} \int_{-\infty}^{\infty} \frac{k^2 e^{iks}}{2\pi i k (k)^j} dk \qquad j = 0,1,2 \qquad \text{(A24)}$$

$$J_j = q_{rs} d_j \frac{U^2}{b^2} \int_{-\infty}^{\infty} \frac{(F + iG) k^2 e^{iks}}{2\pi i k (k)^j} dk \qquad j = 0,1,2 \qquad \text{(A25)}$$

Remembering also that

$$\int_{-\infty}^{\infty} \frac{e^{iks}}{2\pi i k} dk = H(s) \leftarrow \text{unit step function}$$

$$\int_{-\infty}^{\infty} \frac{(F + iG) e^{iks}}{2\pi i k} dk = \phi(s) \leftarrow \text{Wagner function}$$

eqns. (A24) and (A25) yield the following results:

$$
\begin{aligned}
I_o &= -a_o \ddot{q}_{rs} \\
J_o &= -d_o \phi(s) \ddot{q}_{rs} \\
I_1 &= -i\, a_1 \frac{U}{b} \dot{q}_{rs} \\
J_1 &= -i\, d_1 \frac{U}{b} \phi(s) \dot{q}_{rs} \\
I_2 &= a_2 \frac{U^2}{b^2}\, q_{rs} \\
J_2 &= d_2 \frac{U^2}{b^2}\, \phi(s) q_{rs}
\end{aligned}
\tag{A26}
$$

where $\dot{q}_{rs}$, $\ddot{q}_{rs}$ represent, respectively, step type variations in velocity and acceleration of the r^{th} generalized coordinate.

In the following, the eqns. for $L_j q_r$ and $M_j q_r$ will be presented (as taken from refs. 15, 16) together with the respective results of step integration, denoted by $(\omega^2 L_j q_r)_s$ and $(\omega^2 M_j q_r)_s$:

$$L_j q_r = \{1 - i \frac{2}{k} (F+iG)\} q_r$$

$$(\omega^2 L_j q_r)_s = - \ddot{q}_{rs} - 2\phi(s) \frac{U}{b} \dot{q}_{rs} \tag{A27}$$

$$L_2 q_r = \{\frac{1}{2} - \frac{i}{k} [1+2(F+iG)] - \frac{2}{k^2} (F+iG)\} q_r$$

$$(\omega^2 L_2 q_r)_s = - \frac{1}{2} \ddot{q}_{rs} - [\frac{U}{b} (1+2\phi(s))] \dot{q}_{rs} - \frac{2U^2}{b^2} \phi(s) q_{rs} \tag{A28}$$

$$L_3 q_r = \{- \frac{T_1}{\pi} + \frac{i}{k} \frac{T_4}{\pi} - \frac{i}{k} \frac{T_{11}}{\pi} (F+iG) - \frac{2}{k^2} \frac{T_{10}}{\pi} (F+iG)\} q_r$$

$$(\omega^2 L_3 q_r)_s = \frac{T_1}{\pi} \ddot{q}_{rs} + \frac{U}{b} (\frac{T_4}{\pi} - \frac{T_{11}}{\pi} \phi(s)) \dot{q}_{rs} - \frac{U^2}{b^2} 2 \frac{T_{10}}{\pi} \phi(s) q_{rs} \tag{A29}$$

$$L_4 q_r = \{- i \frac{2}{k} (F + iG) \frac{\phi_1}{\pi} + \frac{\phi_3}{\pi} \} q_r$$

$$(\omega^2 L_4 q_r)_s = - 2 \frac{U}{b} \frac{\phi_1}{\pi} \phi(s) \dot{q}_{rs} - \frac{\phi_3}{\pi} \ddot{q}_{rs} \tag{A30}$$

$$(\omega^2 L_5 q_r)_s = \frac{T_{1\delta}}{\pi} \ddot{q}_{rs} + \frac{U}{b} (\frac{T_{4\delta}}{\pi} - \frac{T_{11\delta}}{\pi} \phi(s)) \dot{q}_{rs} - \frac{U^2}{b^2} 2 \frac{T_{10\delta}}{\pi} \phi(s) q_{rs} \tag{A31}$$

$$(\omega^2 L_6 q_r)_s = - 2 \frac{U}{b} \frac{\phi_{1\delta}}{\pi} \phi(s) \dot{q}_{rs} - \frac{\phi_{3\delta}}{\pi} \ddot{q}_{rs} \tag{A32}$$

$$M_1 q_r = \frac{1}{2} q_r$$

$$(\omega^2 M_1 q_r)_s = - \frac{1}{2} \ddot{q}_{rs} \tag{A33}$$

$$M_2 q_r = \{\frac{3}{8} - \frac{i}{k}\} q_r$$

$$(\omega^2 M_2 q_r)_s = - \frac{3}{8} \ddot{q}_{rs} - \frac{U}{b} \dot{q}_{rs} \tag{A34}$$

$$M_3 q_r = \{- \frac{T_7}{\pi} - (e + \frac{1}{2}) \frac{T_1}{\pi} + \frac{i}{k} (\frac{2p + T_4}{\pi}) - \frac{1}{k^2} (\frac{T_4 + T_{10}}{\pi}) \} q_r$$

$$(\omega^2 M_3 q_r)_s = [\frac{T_7}{\pi} + (e + \frac{1}{2}) \frac{T_1}{\pi}] \ddot{q}_{rs} + \frac{U}{b} (\frac{2p + T_4}{\pi}) \dot{q}_{rs} - (\frac{T_4 + T_{10}}{\pi}) q_{rs} \tag{A35}$$

$$M_4 q_r = \{- \frac{i}{k} \frac{\phi_5}{\pi} + \frac{1}{4} \frac{\phi_6}{\pi} \} q_r$$

$$(\omega^2 M_4 q_r)_s = - \frac{U}{b} \frac{\phi_5}{\pi} \dot{q}_{rs} - \frac{\phi_6}{4\pi} \ddot{q}_{rs} \tag{A36}$$

$$(\omega^2 M_5 q_r)_s = \left[\frac{T_{7\delta}}{\pi} + \left(e_\delta + \frac{1}{2}\right)\frac{T_{1\delta}}{\pi}\right]\ddot{q}_{rs} + \frac{U}{b}\left(\frac{2p_\delta + T_{4\delta}}{\pi}\right)\dot{q}_{rs} - \frac{U^2}{b^2}\left(\frac{T_{4\delta} + T_{10\delta}}{\pi}\right)q_{rs} \quad \text{(A37)}$$

$$(\omega^2 M_6 q_r)_s = -\frac{U}{b}\frac{\phi_{5\delta}}{\pi}\dot{q}_{rs} - \frac{\phi_{6\delta}}{4\pi}\ddot{q}_{rs} \quad \text{(A38)}$$

Substituting eqns. (A27) - (A38) into the second term of eqn. (A20) we obtain the contribution of the controls to the generalized step forces. This can be written in the form

$$\begin{Bmatrix} Q_{h/b} \\ Q_\alpha \end{Bmatrix}_s = \pi\rho b^2 U^2 (\phi(s)[A_1] + [A_2]) \begin{Bmatrix} \beta_s \\ \delta_s \end{Bmatrix} + \pi\rho b^3 U (\phi(s)[B_1] + [B_2]) \begin{Bmatrix} \dot{\beta}_s \\ \dot{\delta}_s \end{Bmatrix} + \pi\rho b^4 [E] \begin{Bmatrix} \ddot{\beta}_s \\ \ddot{\delta}_s \end{Bmatrix} \quad \text{(A39)}$$

where

$$[A_1] = \begin{bmatrix} \left[-2 + 2\frac{T_{10}}{\pi}\right] & 2\,T_{10\delta} \\ \frac{\ell_1}{b}\left(-2 + 2\frac{T_{10}}{\pi}\right) & 2\frac{\ell_1}{b}\frac{T_{10\delta}}{\pi} \end{bmatrix} \quad \text{(A40)}$$

$$[A_2] = \begin{bmatrix} 0 & 0 \\ -\left(\frac{T_4 + T_{10}}{\pi}\right) & -\left(\frac{T_{4\delta} + T_{10\delta}}{\pi}\right) \end{bmatrix} \quad \text{(A41)}$$

$$[B_1] = \begin{bmatrix} [\frac{2\ell_4}{b} - 2 + \frac{T_{11}}{\pi} + \frac{2\phi_1}{\pi} \frac{(\ell_2 - \ell_4)}{b}] [\frac{T_{11\delta}}{\pi} - \frac{2\phi_{1\delta}}{\pi} \frac{\ell_3}{b}] \\ [\frac{\ell_1}{b} (\frac{2\ell_4}{b} - 2 + \frac{T_{11}}{\pi} + \frac{2\phi_1}{\pi} \frac{(\ell_2 - \ell_4)}{b}] [\frac{\ell_1}{b} (\frac{T_{11\delta}}{\pi} - \frac{2\phi_{1\delta}}{\pi} \frac{\ell_3}{b})] \end{bmatrix} \quad \text{(A42)}$$

$$[B_2] = \begin{bmatrix} B_2(1,1) & B_2(1,2) \\ B_2(2,1) & B_2(2,2) \end{bmatrix}$$

where

$$B_2(1,1) = -1 - \frac{T_4}{\pi}$$

$$B_2(1,2) = -\frac{T_{4\delta}}{\pi}$$

$$B_2(2,1) = -\frac{\ell_1}{b} (1 + \frac{T_4}{\pi}) + 1 + \frac{(2p + T_4)}{\pi} - \frac{\phi_5}{\pi} \frac{(\ell_2 - \ell_4)}{b}$$

$$B_2(2,2) = -\frac{\ell_1}{b} \frac{T_{4\delta}}{\pi} + \frac{(2p_\delta + T_{4\delta})}{\pi} + \frac{\phi_{5\delta}}{\pi} \frac{\ell_3}{b}$$

$$[E] = \begin{bmatrix} E(1,1) & E(1,2) \\ E(2,1) & E(2,2) \end{bmatrix}$$

where

$$E(1,1) = \frac{\ell_4}{b} - \frac{1}{2} - \frac{T_1}{\pi} \frac{\phi_3}{\pi} \frac{(\ell_2 - \ell_4)}{b}$$

$$E(1,2) = -\frac{T_{1\delta}}{\pi} - \frac{\phi_{3\delta}}{\pi} \frac{\ell_3}{b}$$

$$E(2,1) = \frac{\ell_1}{b} [\frac{\ell_4}{b} - \frac{1}{2} - \frac{T_1}{\pi} + \frac{\phi_3}{\pi} \frac{(\ell_2 - \ell_4)}{b}] - \frac{1}{2} \frac{\ell_4}{b} + \frac{3}{8} + \frac{T_7}{\pi} + (e + \frac{1}{2}) \frac{T_1}{\pi} - \frac{\phi_6}{4\pi} \frac{(\ell_2 - \ell_4)}{b}$$

$$E(2,2) = \frac{\ell_1}{b} (-\frac{T_{1\delta}}{\pi} - \frac{\phi_{3\delta}}{\pi} \frac{\ell_3}{b}) + \frac{T_{7\delta}}{\pi} + (e_\delta + \frac{1}{2}) \frac{T_{1\delta}}{\pi} + \frac{\phi_{6\delta}}{4\pi} \frac{\ell_3}{b} \quad \text{(A44)}$$

It is important to note here that unlike ref. 13 h/b is taken to be positive in the upwards direction. This requires a change of sign of the first column of each of the optimized matrices [C] and [G] which appear in ref. 13.

REFERENCES

1. Davis, H.M., Swaim, R.L.: Controlling Dynamic Response in Rough Air. AIAA Pap. No. 66-997, Nov. - Dec. 1966.

2. Wykes, J.H.; Mori, A.S.: Techniques and Results of an Analytical Investigation into Controlling the Structural Modes of a Flexible Aircraft. AIAA Symposium on Structural Dynamics and Aeroelasticity, Aug. - Sept. 1965, pp. 419 - 433.

3. Wykes, J.H.; Mori, A.S.: An Analysis of Flexible Aircraft Structural Mode Control. AFFDL TR 65-190, Part I, June 1966.

4. Dempster, J.B.; Roger, K.L.: Evaluation of B-52 Structural Response to Random Turbulence with Stability Augmentation Systems. JAC, Nov.-Dec. 1967.

5. Rohling, W.J.: Flying Qualities - An Integral Part of a Stability Augmentation System. JAC, Nov. - Dec. 1969.

6. Dempster, J.B.; Arnold, J.I.: Flight Test Evaluation of an Advanced Stability Augmentation System for the B-52 Aircraft. AIAA Pap. No. 68-1068, Oct. 1968.

7. Thompson, G.O.; Kass, G.J.: Active Flutter Suppression - An Emerging Technology. Pap. No. 7-B2 of the Joint Automatic Control Conference of the AACC, August 1971.

8. Topp, L.J.: Potential Performance Gains by Use of a Flutter Suppression System. Pap. No. 7-B3 of the Joint Automatic Control Conference of the AAC, August 1971.

9. Abel, I.; Sanford, M.C.: Status of Two Studies on Active Control of Aeroelastic Response. NASA TM X-2909, Sept. 1973.

10. Broadbent, E.G.; Williams, M.: The Effect of Structural Damping on Binary Flutter. R&M. 3169, British A.R.C., 1960.

11. Nissim, E.: The Effect of Linear Damping on Flutter Speed. Part I: Binary Systems. Part II: Systems with Three of More Degrees of Freedom. Aeronaut. Quart. Vol. XVI, May and Aug. 1965.

12. Done, G.T.S.: The Effect of Linear Damping on Flutter Speed. R&M. No. 3396, British A.R.C., 1965.

13. Nissim, E.: Flutter Suppression Using Active Controls Based on the Concept of Aerodynamic Energy. NASA TN D-6199, March 1971.

14. Garrick, I.E.: Perspectives in Aeroelasticity. Proceedings of the 14^{th} Israel Annual Conference on Aviation and Astronautics, March 1972.

15. Smilg, B.; Wasserman, L.S.: Application of Three Dimensional Flutter Theory to Aircraft Structures. ACTR No. 4798, Material Div., Army Air Corps, July 1942.

16. Wasserman, L.S.; Mykytow, W.J.; Spielberg, I.: Tab Flutter Theory and Applications. AAF TR No. 5153, Air Technical Service Command, Army Air Forces, Sept. 1944.

TABLE I - MINIMUM VALUES OF ω_r FOR THE ARAVA STOL TRANSPORT

STN No.	1	2	3	4	5	6	7	8	9	10
$(\omega_r)_{min}$	2.50	2.31	2.12	1.93	1.75	1.50	1.25	1.0	1.0	1.0

TABLE II - MINIMUM VALUES OF ω_r FOR THE WESTWIND BUSINESS JET TRANSPORT

STN No.	1	2	3	4	5	6	7	8	9	10
$(\omega_r)_{min}$	6.40	5.75	5.08	4.42	3.82	3.22	3.04	2.86	2.68	2.50

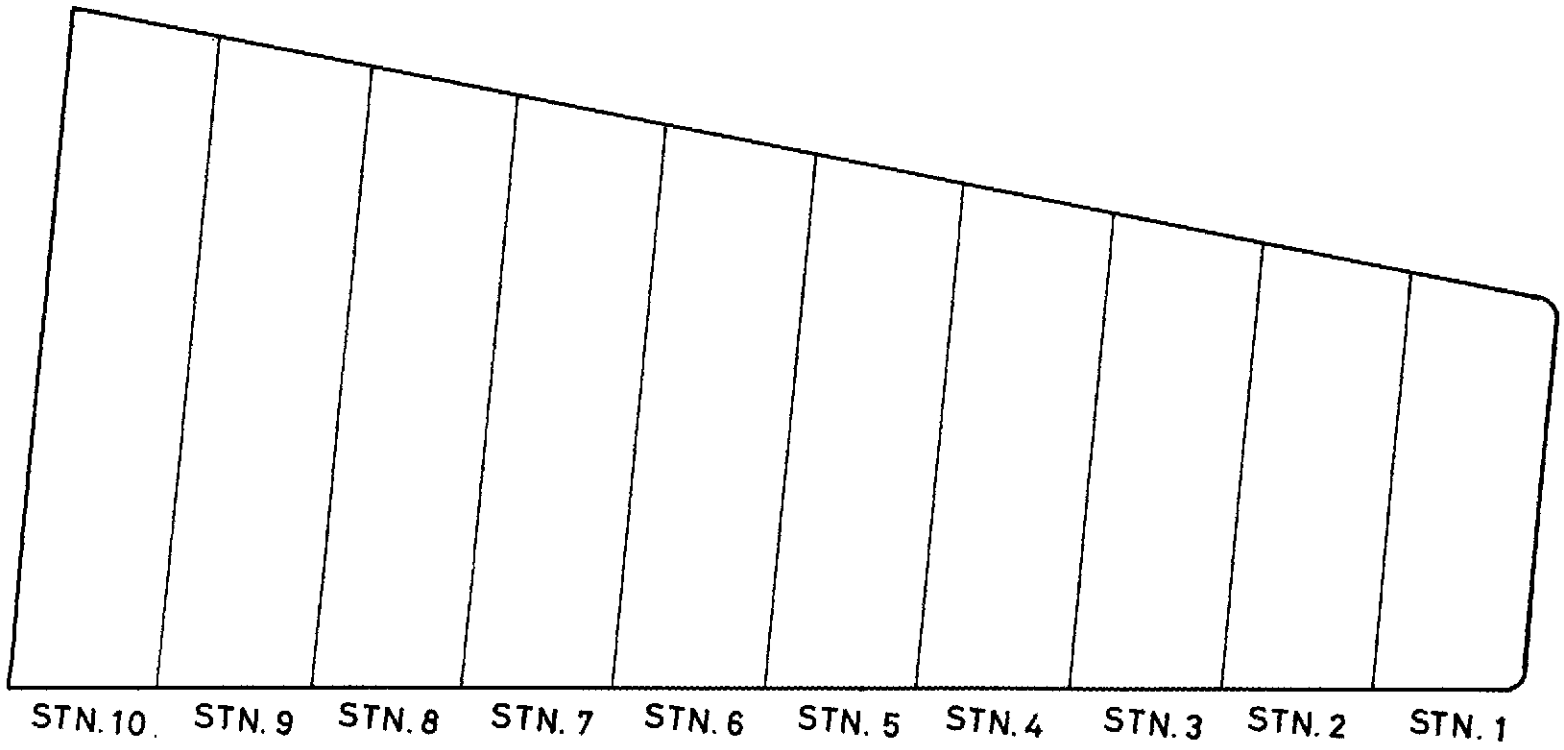

Figure 1: Typical allocation of 10 equal - span stations along the wing.

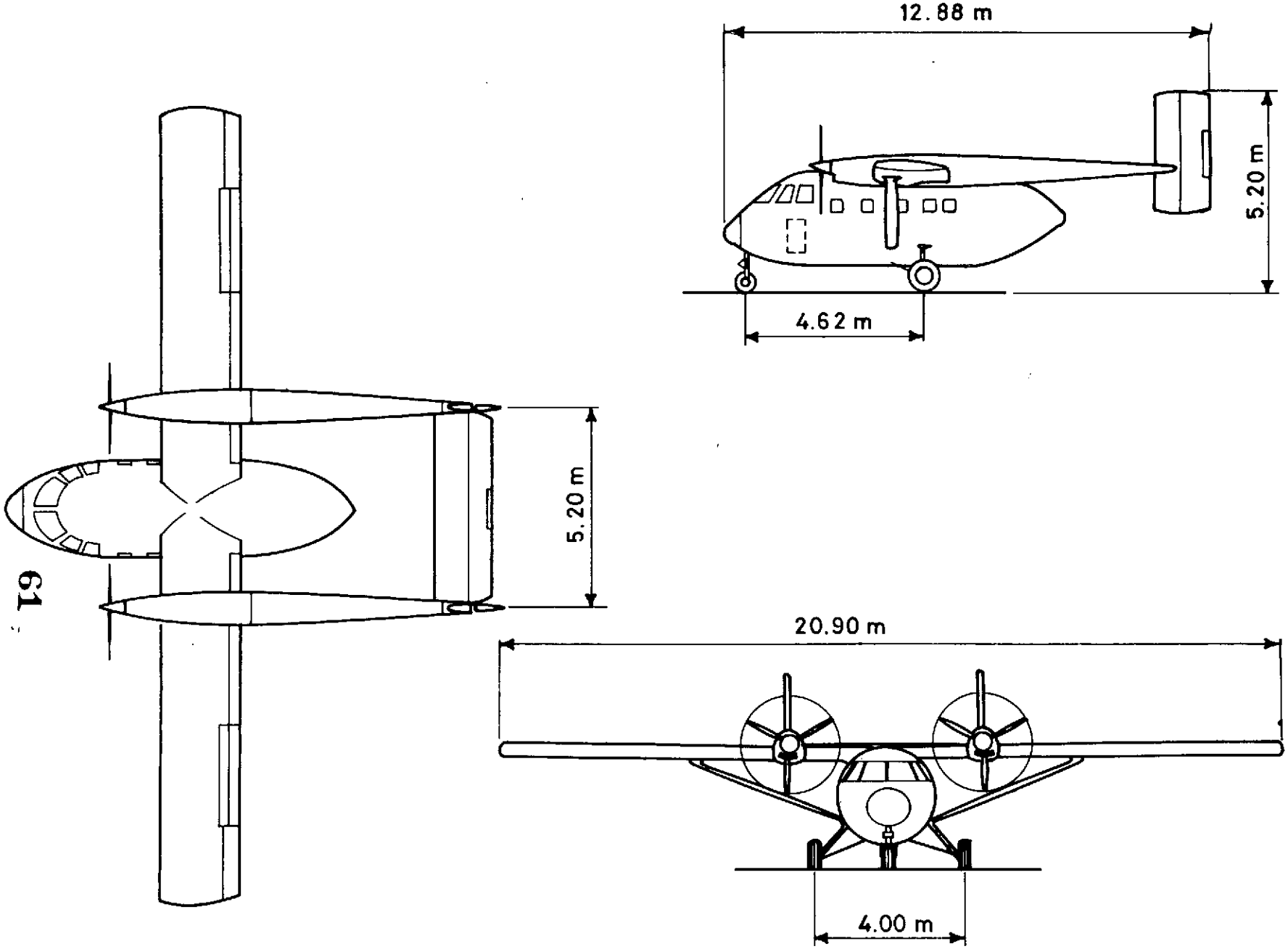

Figure 2: General view and dimensions of the Arava STOL transport.

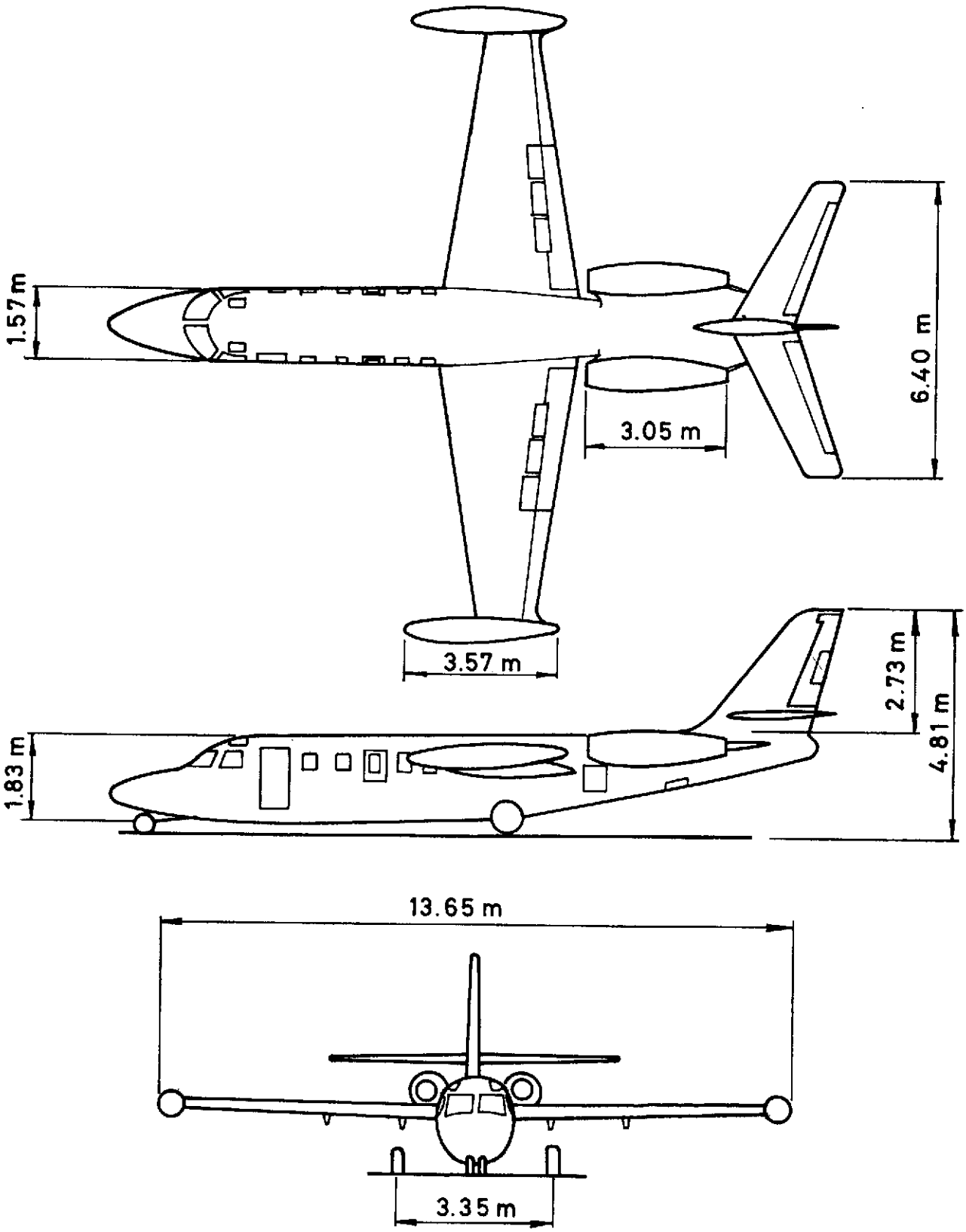

Figure 3: General view and dimensions of the Westwind buisiness jet transport.

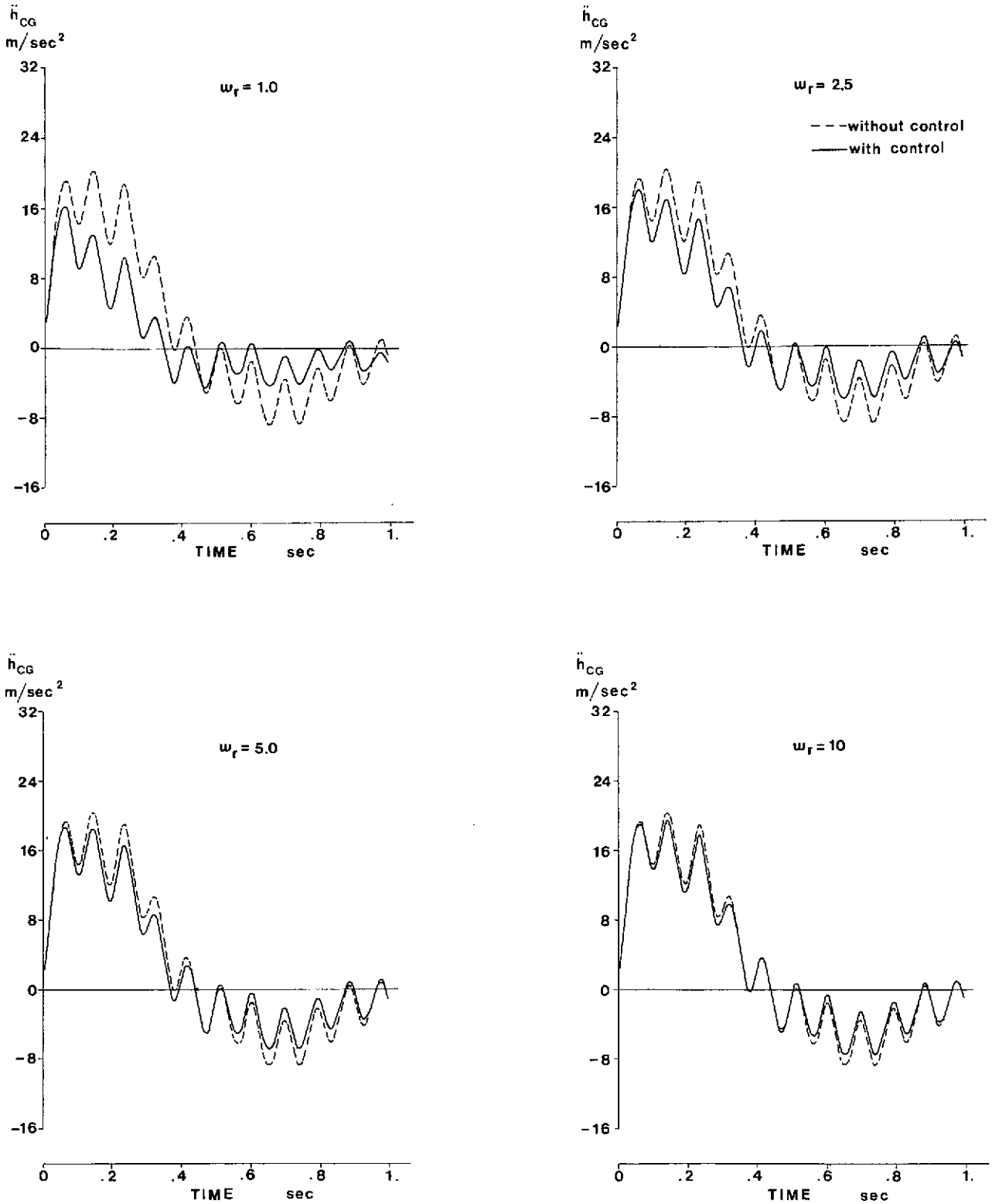

Figure 4: Variation with time of the linear acceleration at c.g. due to a step upgust - Arava transport with a single L.E. - T.E. active system located at station 10 and having different values of ω_r.

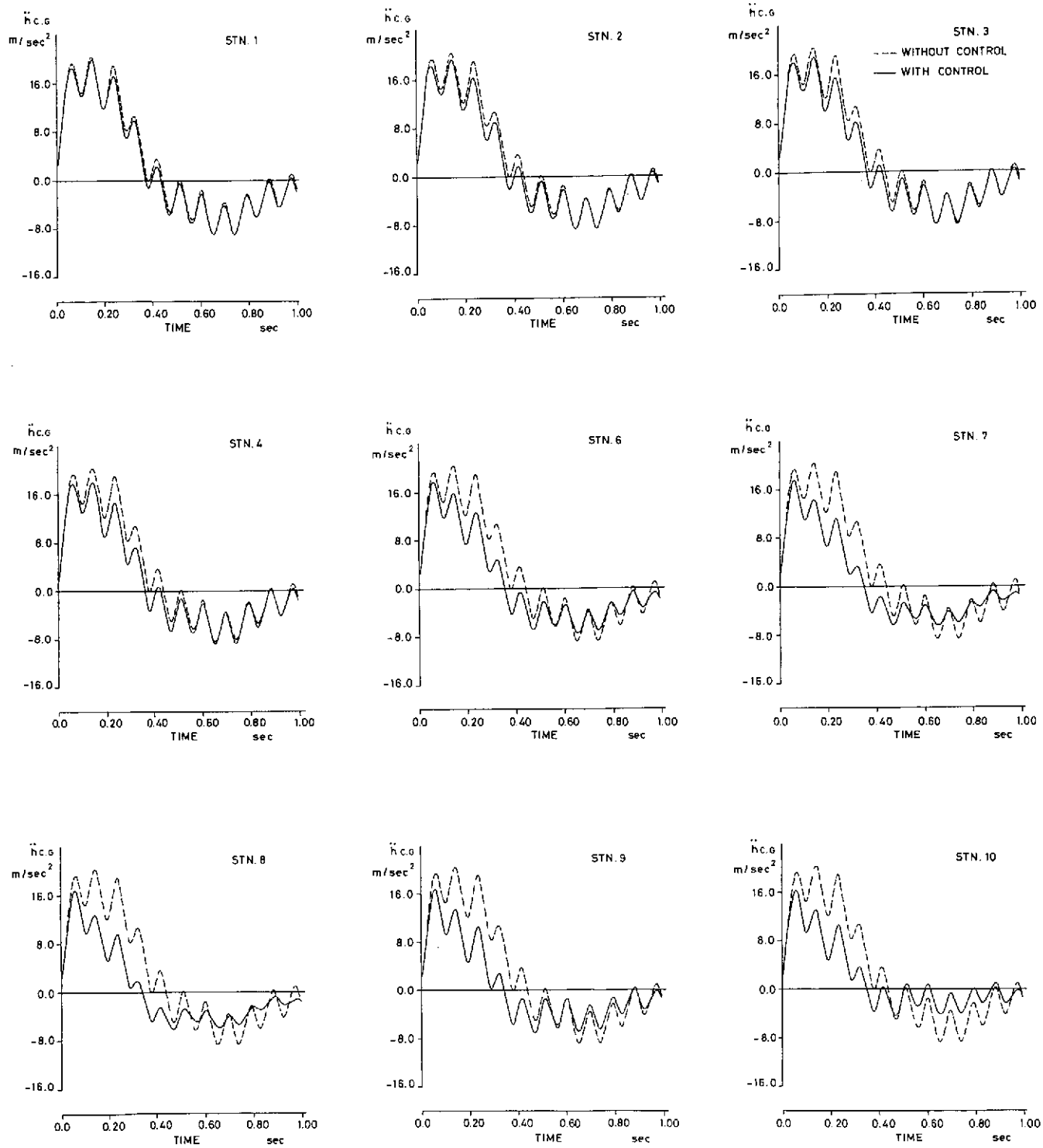

Figure 5: Variation with time of the linear acceleration at c.g. due to a step up just - Arava transport with a single L. E. - T. E. active system located at various stations along the wing.

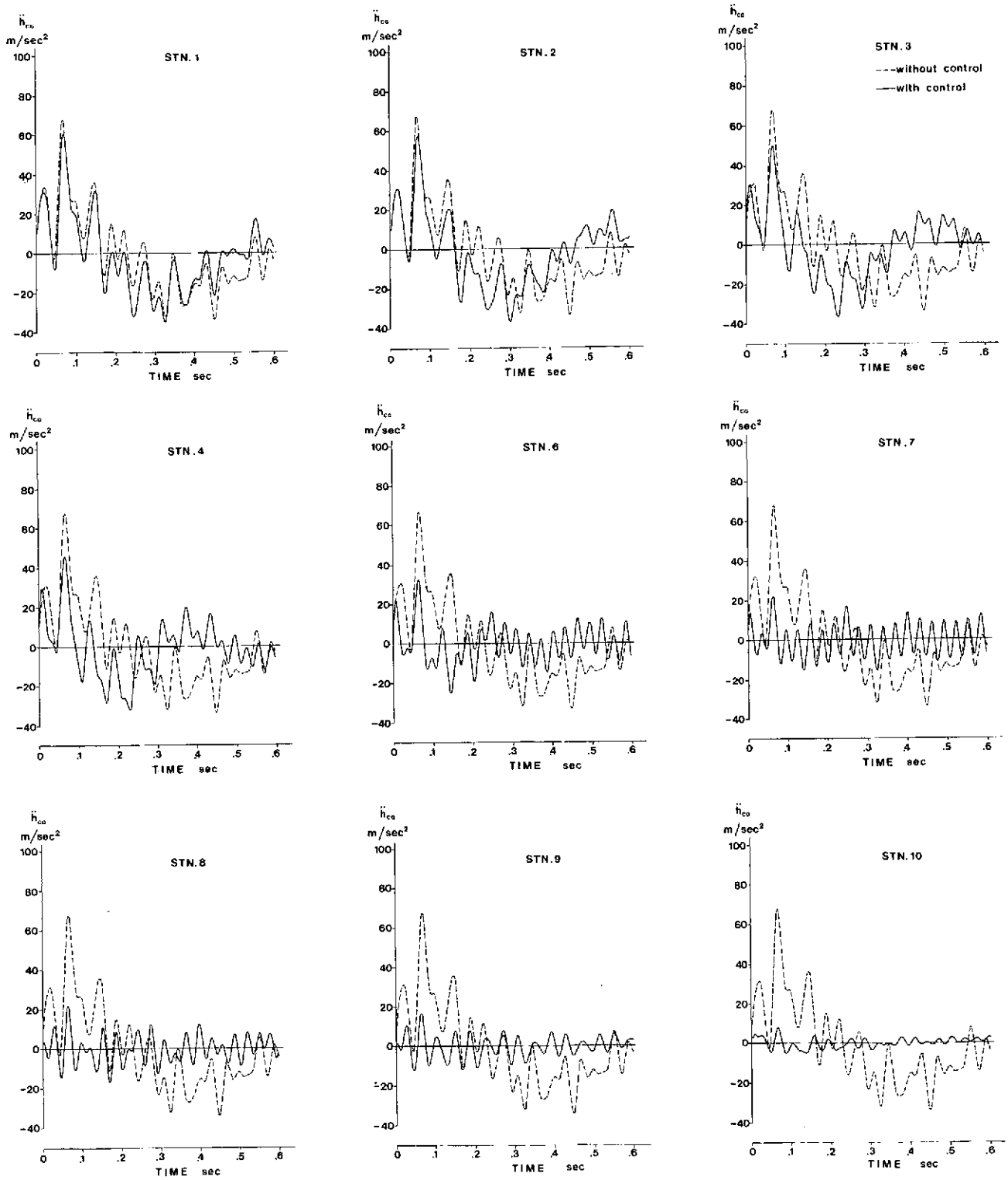

Figure 6: Variation with time of the linear acceleration at c.g. due to a step up gust - Westwind transport with a single L.E. - T.E. active system located at various stations along the wing.

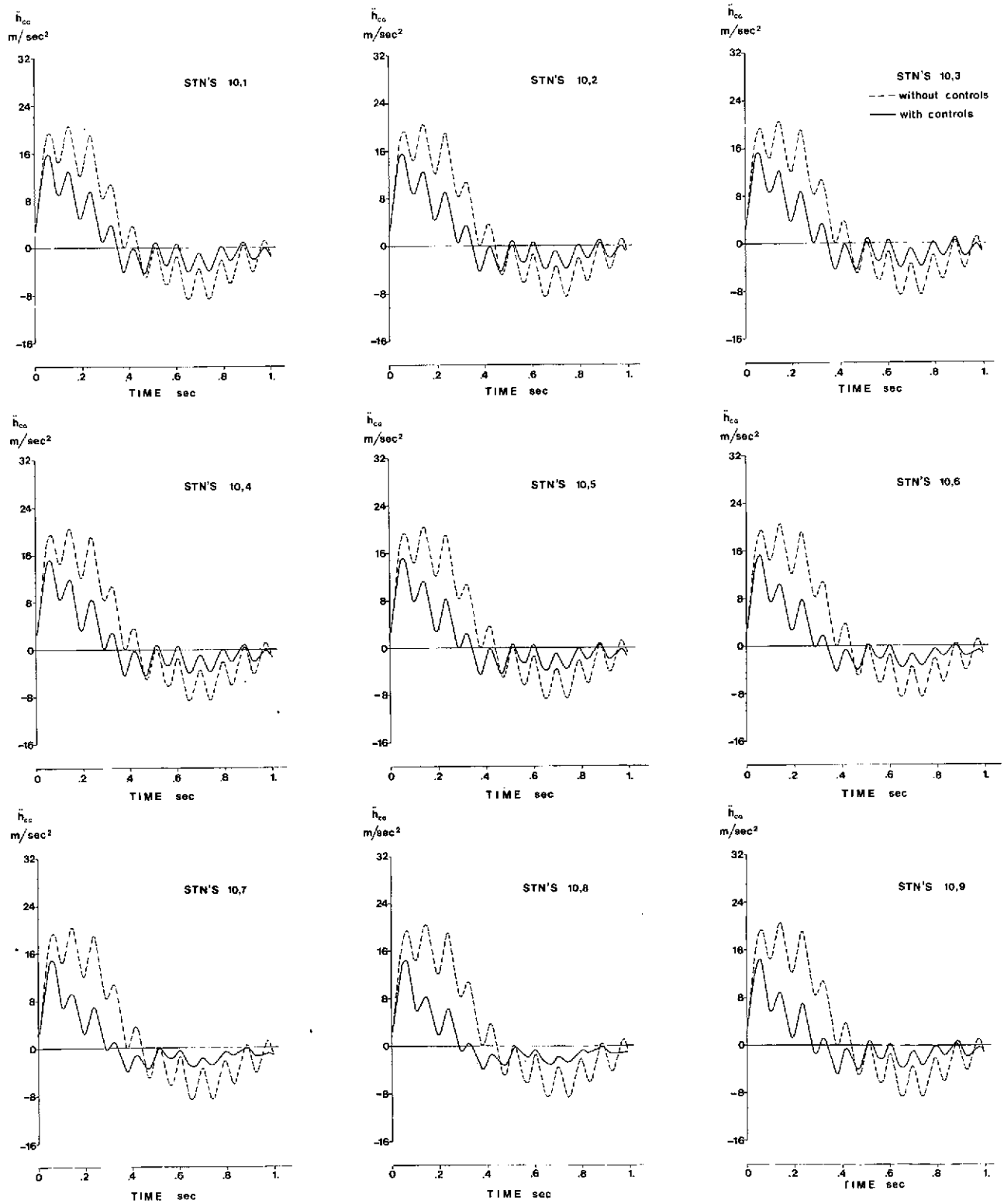

Figure 7: Variation with time of the linear acceleration at c.g. due to a step up gust - Arava transport with 2 L.E. - T.E. active systems: one located at station 10 and one located at various stations along the wing.

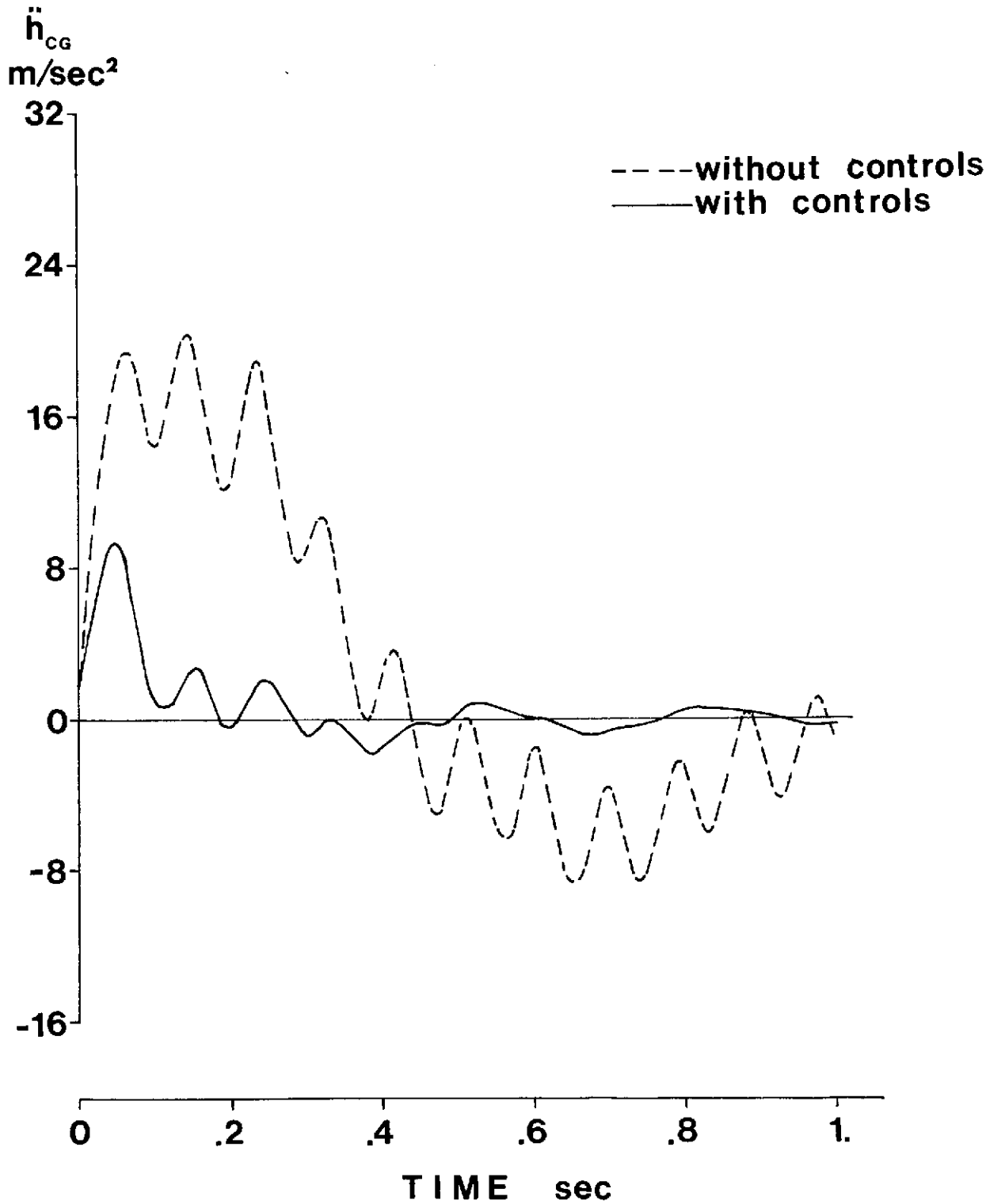

Figure 8: Variation with time of the linear acceleration at c.g. due to a step up gust - Arava transport with 10 L.E. - T.E. active systems spanning the whole of the wing.

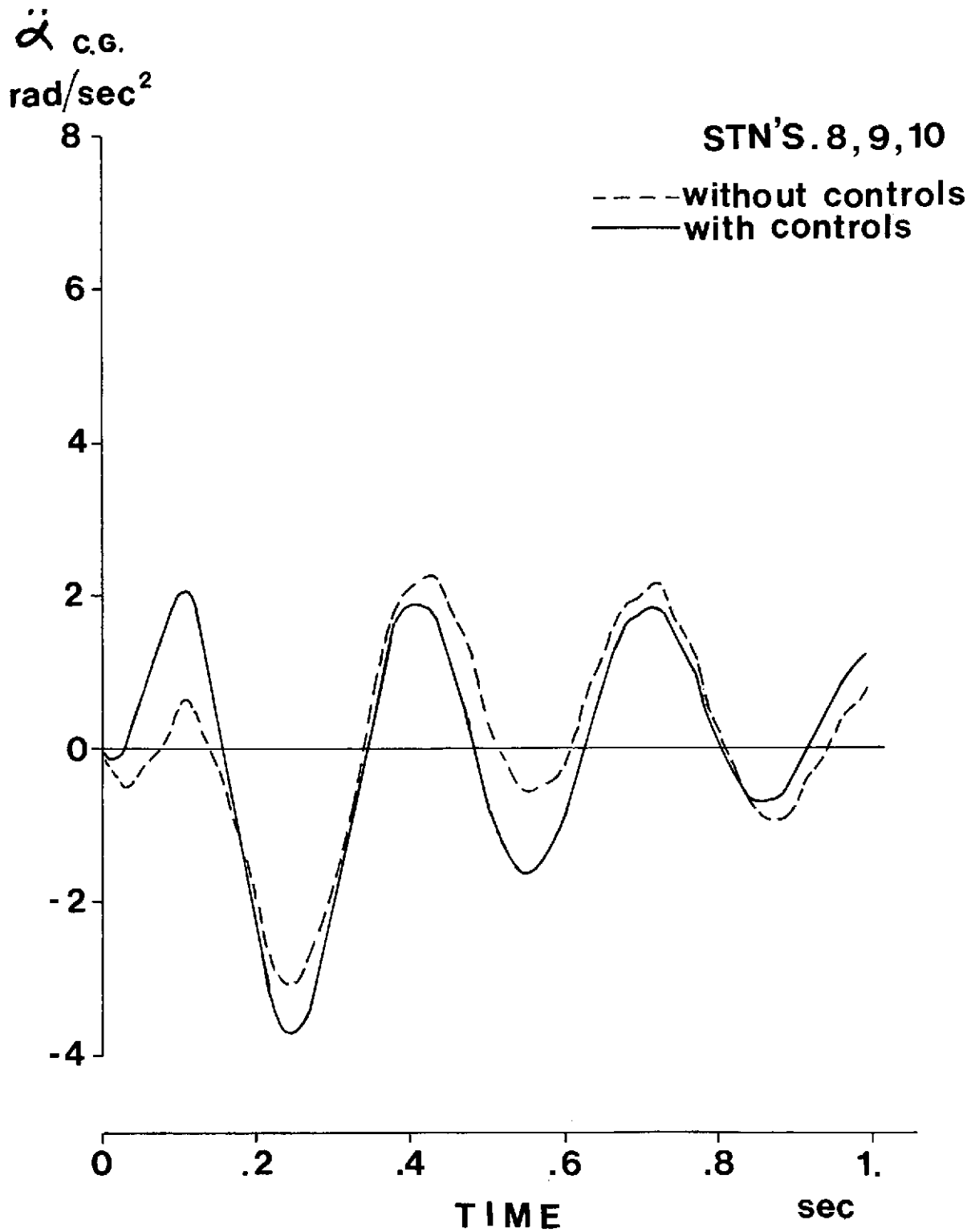

Figure 9: Variation with time of the angular acceleration at c.g. due to a step up gust - Arava transport with 3 L.E. - T.E. active systems located at stations 8, 9 and 10.

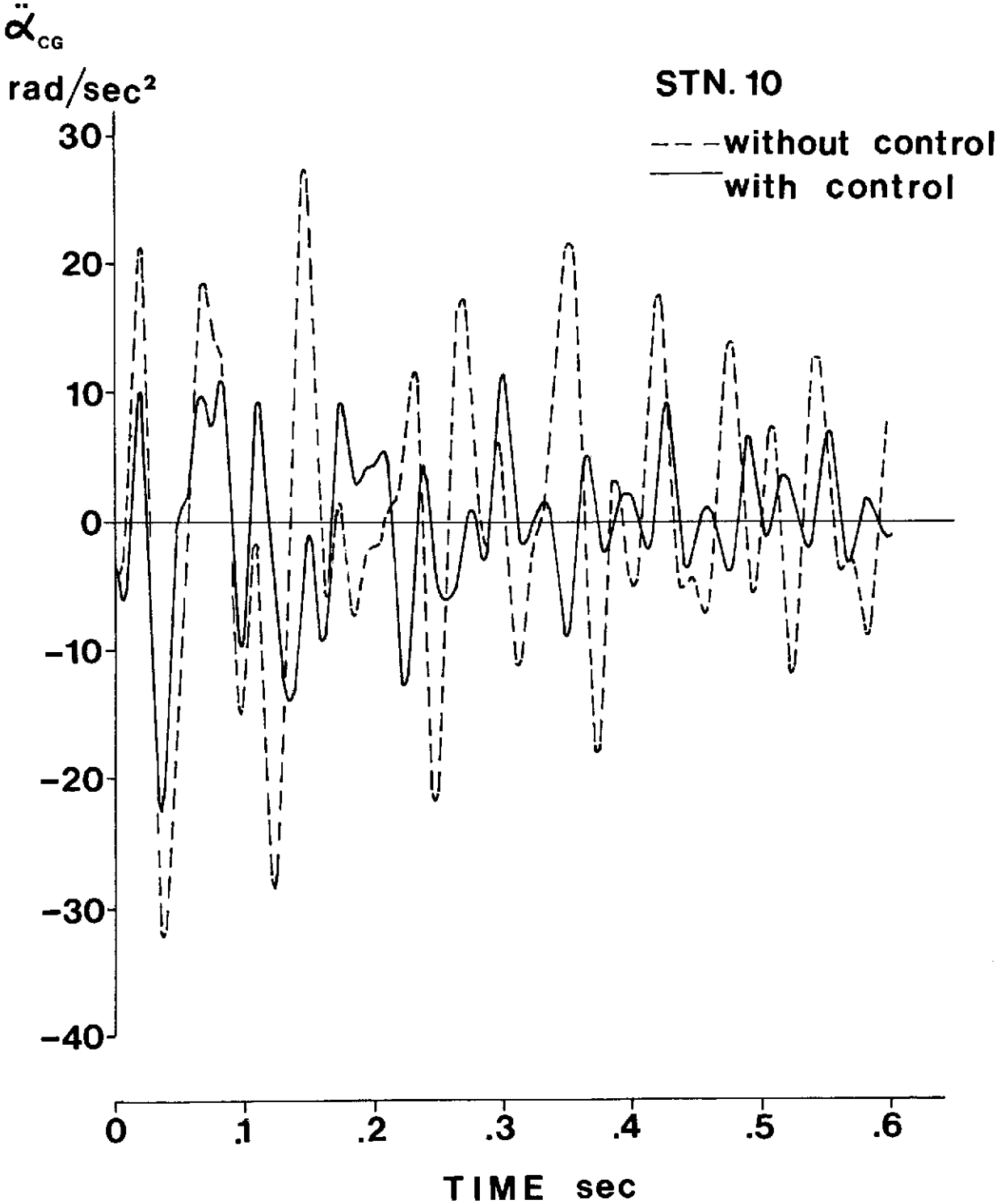

Figure 10: Variation with time of the angular acceleration at c.g. due to a step up gust - Westwind transport with a single L.E. - T.E. active system located at station 10

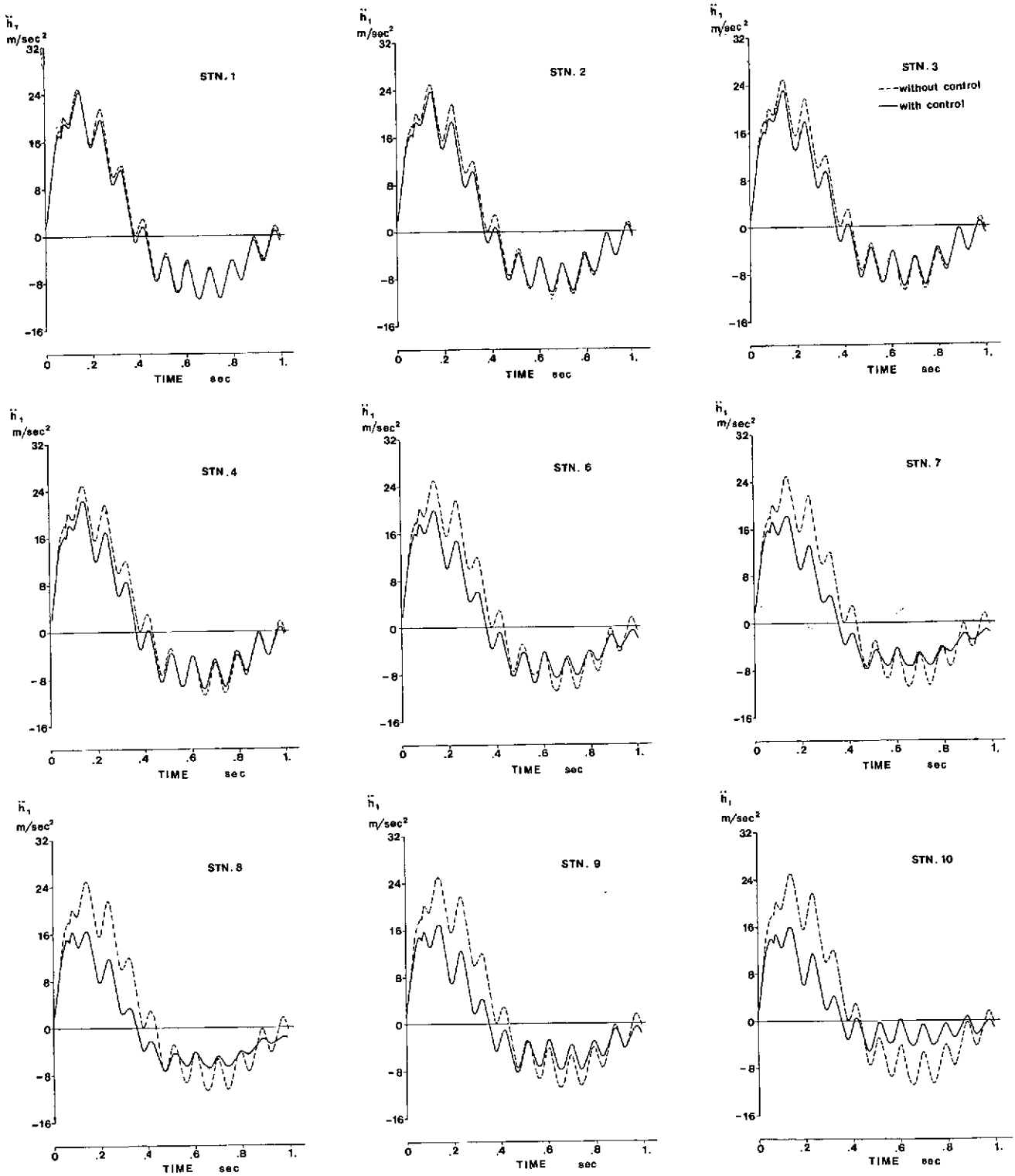

Figure 11: Variation with time of the linear acceleration of Point 1 due to a step up gust - Arava transport with a single L.E. - T.E. active system located at various stations along the wing.

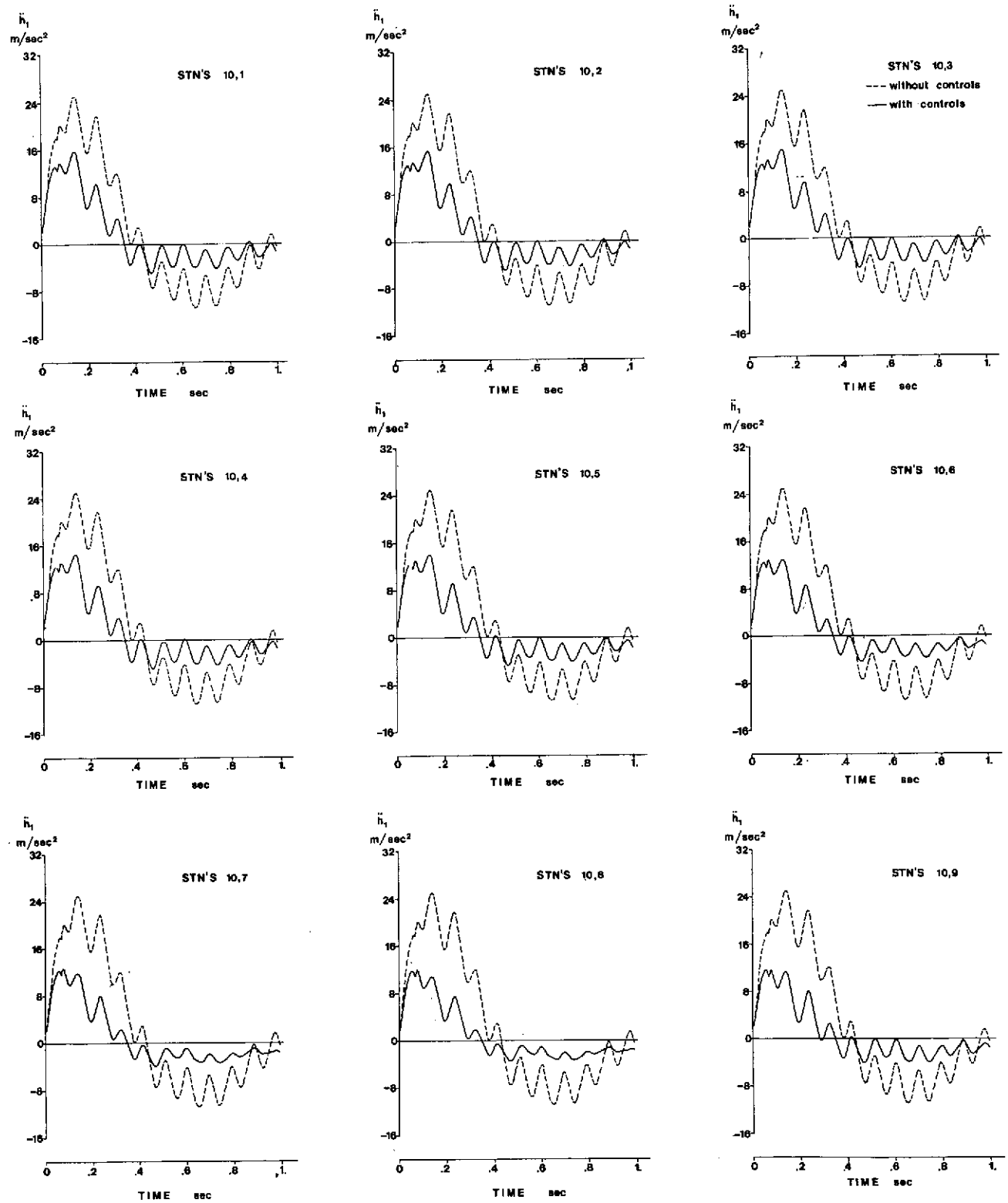

Figure 12: Variation with time of the linear acceleration at Point 1 due to a step up gust - Arava transport with 2 L.E. - T.E. active systems: one located at station 10 and one located at various stations along the wing.

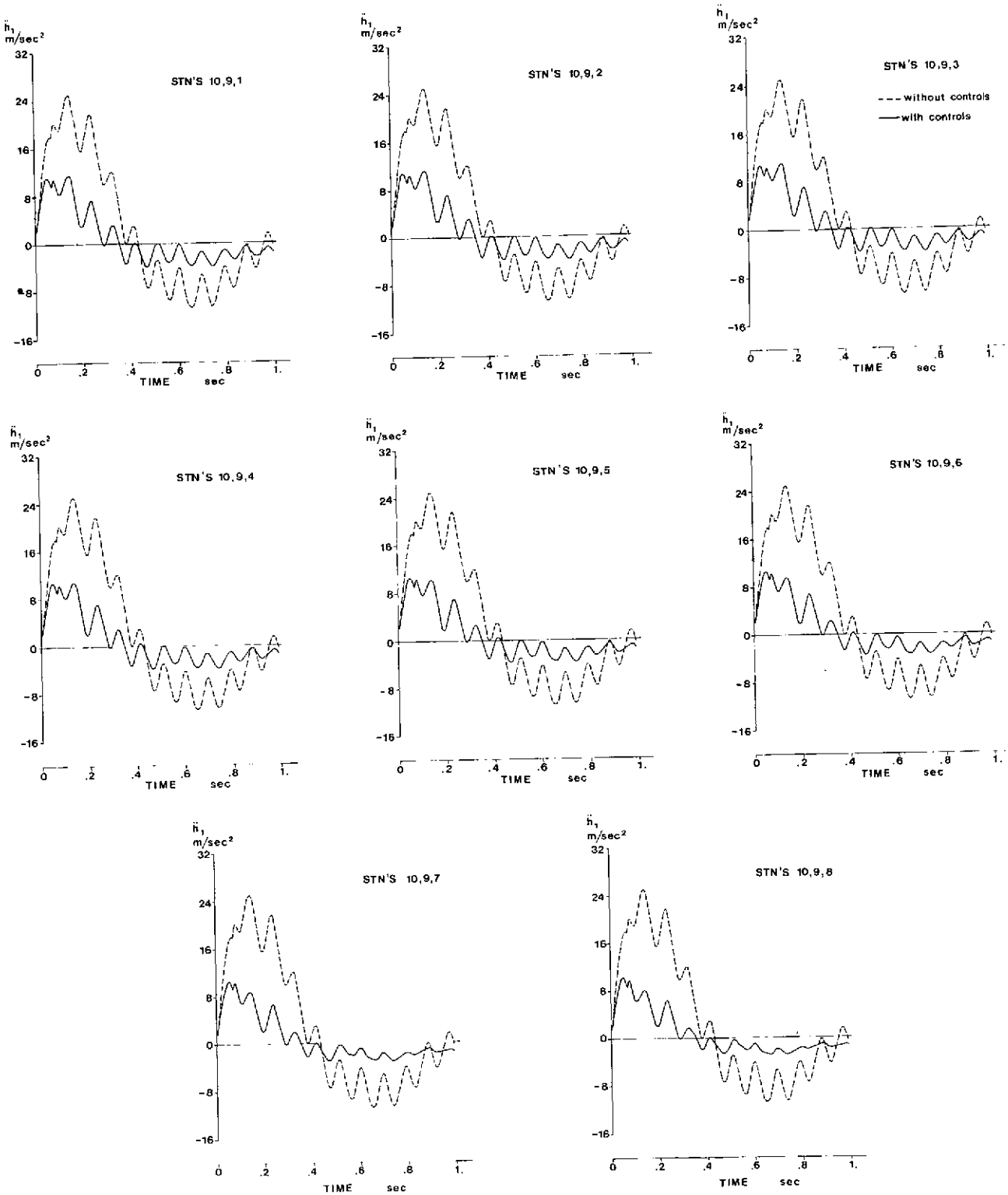

Figure 13. Variation with time of the linear acceleration at Point 1 due to a step up gust - Arava transport with 3 L.E. - T.E. active systems: two located at stations 9 and 10 and one located at various stations along the wing.

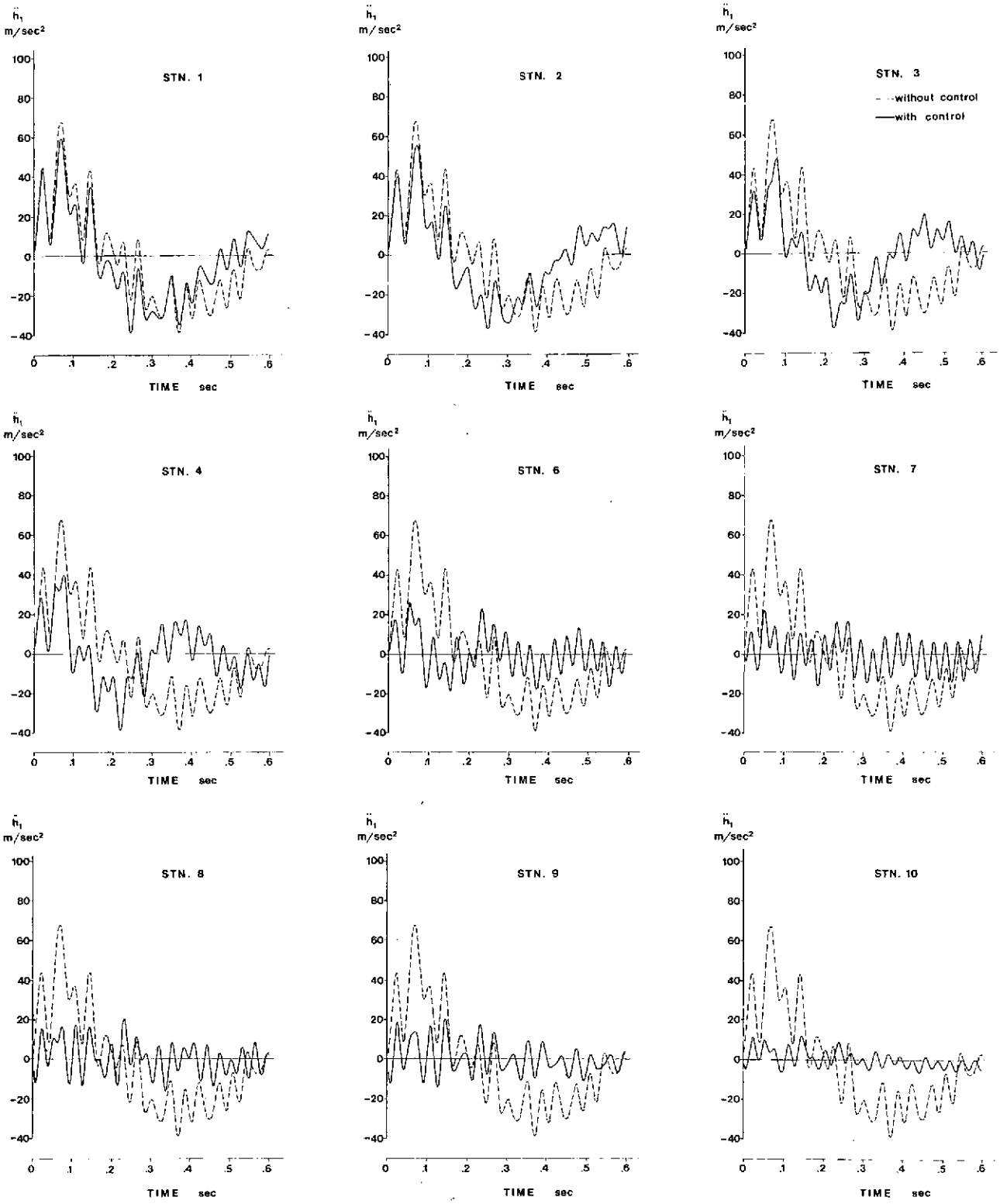

Figure 14: Variation with time of the linear acceleration at Point 1 due to a step up gust - Westwind trasport with a single L.E. - T.E. active system located at various stations along the wing.

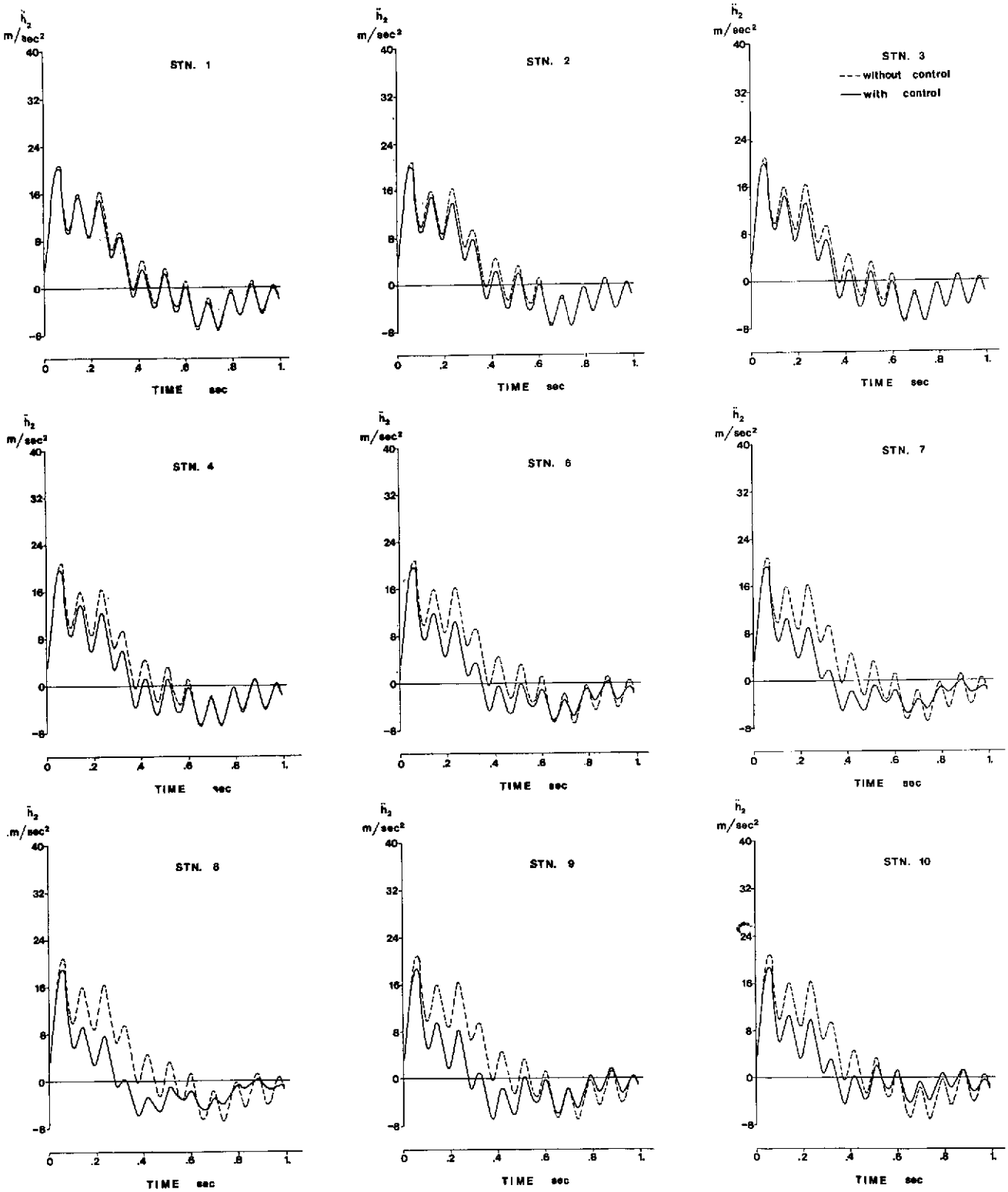

Figure 15: Variation with time of the linear acceleration at Point 2 due to a step up gust - Arava transport with a single L.E. - T.E. active system located at various stations along the wing.

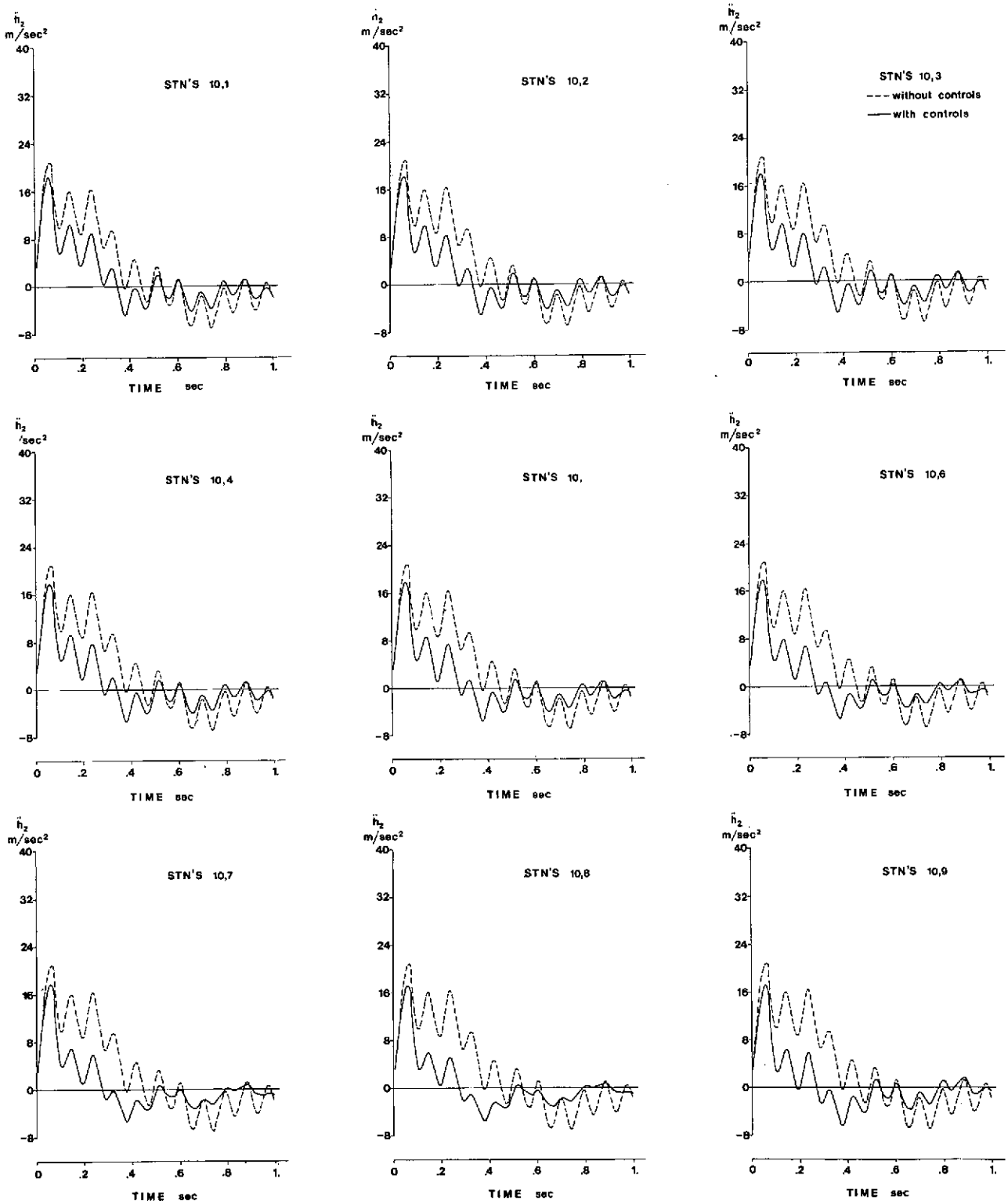

Figure 16: Variation with time of the linear acceleration at Point 2 due to a step up gust - Arava transport with 2 L.E. - T.E. active systems: one located at station 10 and one located at various stations along the wing.

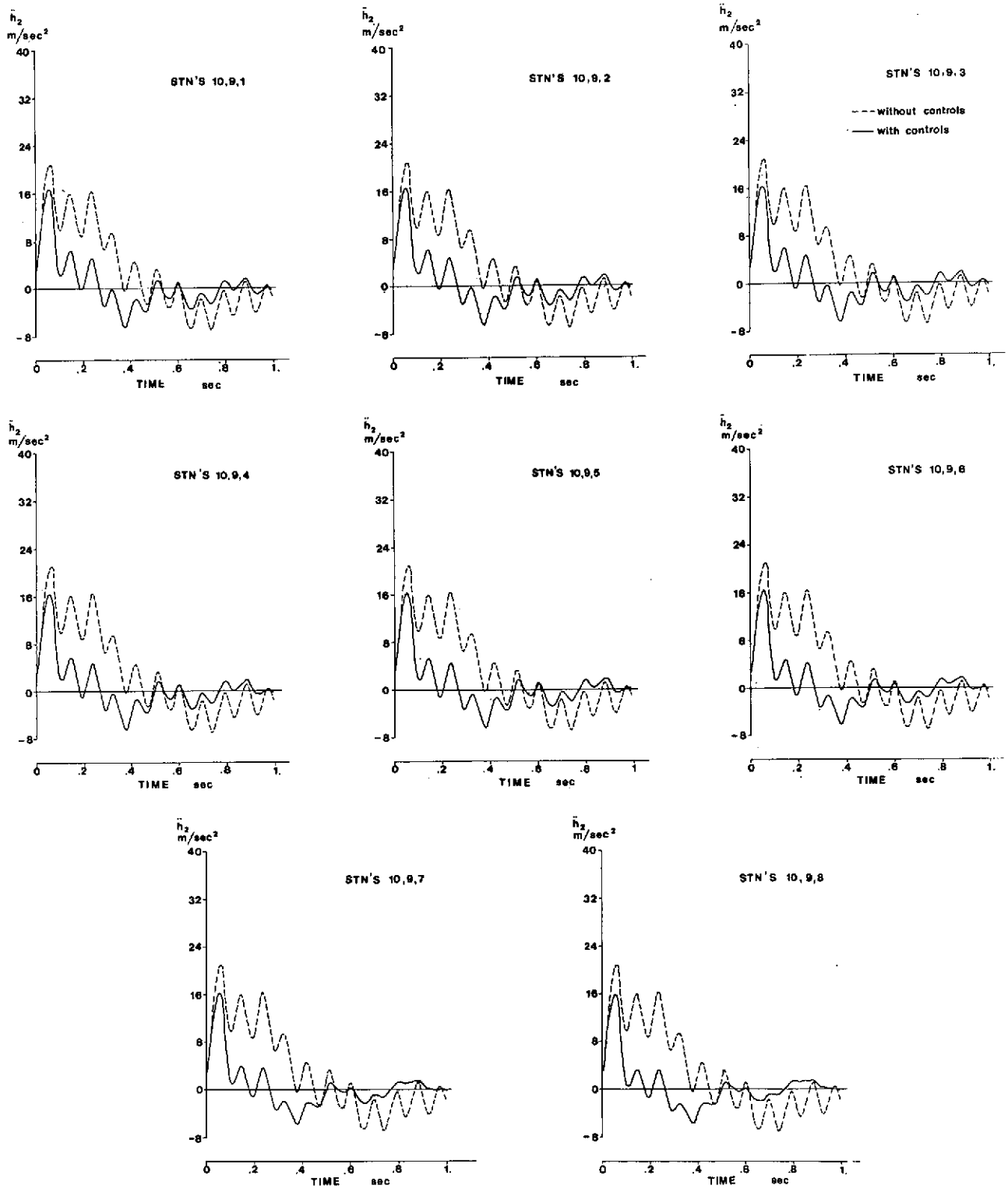

Figure 17: Variation with time of the linear acceleration at Point 2 due to a step up gust - Arava transport with 3 L.E. - T.E. active systems: two located at stations 9 and 10 and one located at various stations along the wing.

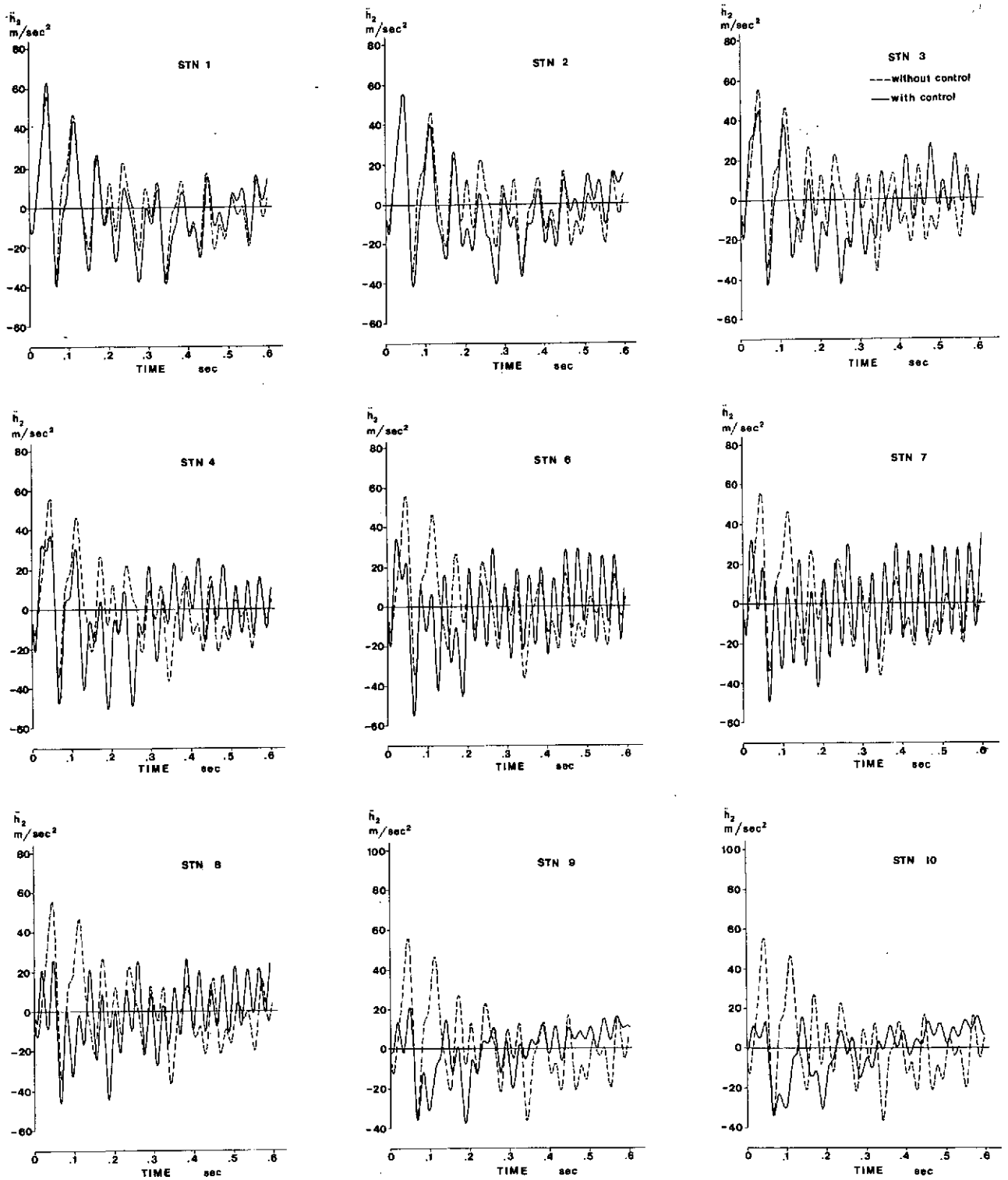

Figure 18: Variation with time of the linear acceleration at Point 2 due to a step up gust - Westwind transport with a single L.E. - T.E. active system located at various stations along the wing.

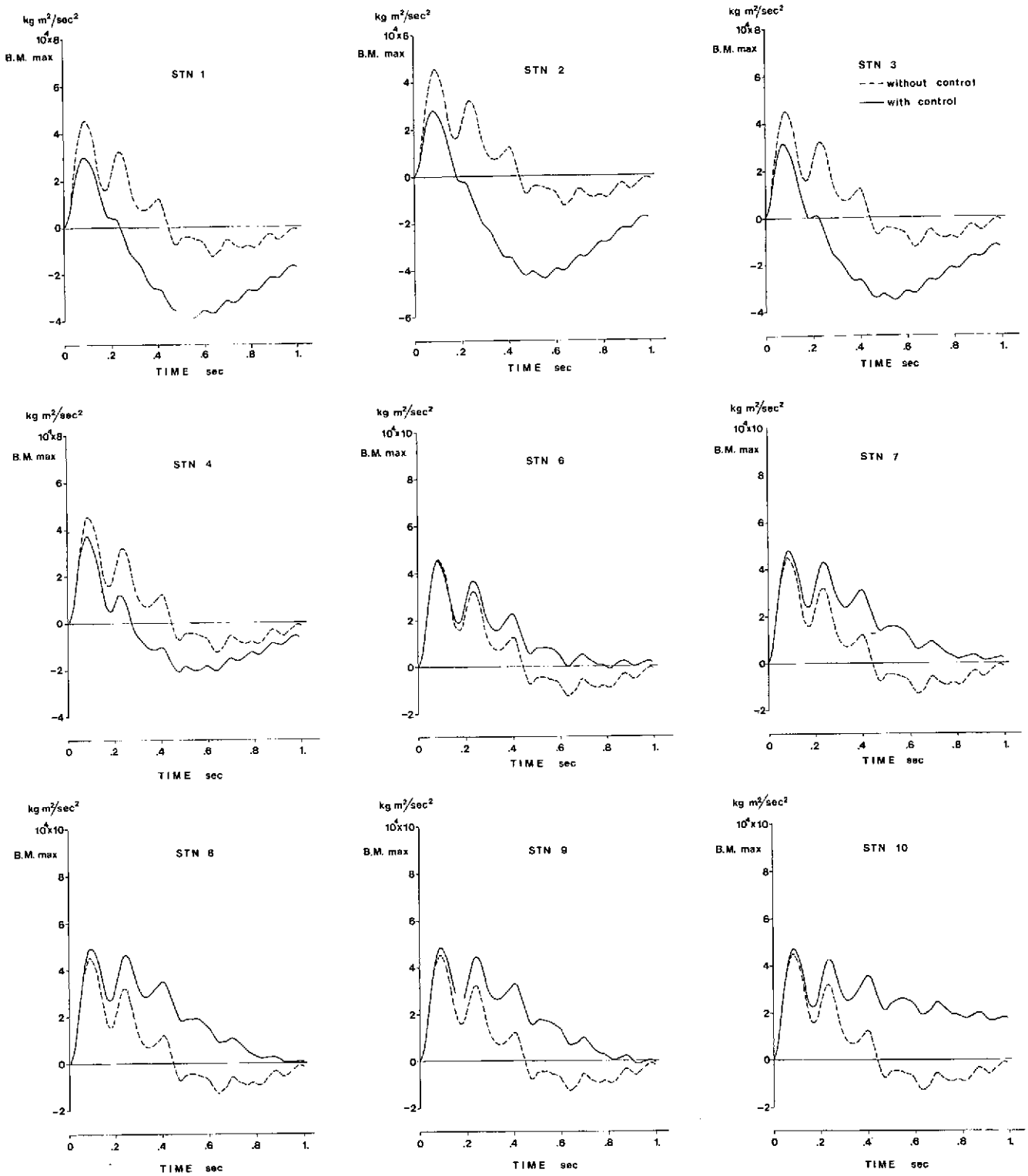

Figure 19: Variation with time of the maximum wing bending moment (at station 5) due to a step up gust - Arava transport with a single L - T.E. active system located at various stations along the wing.

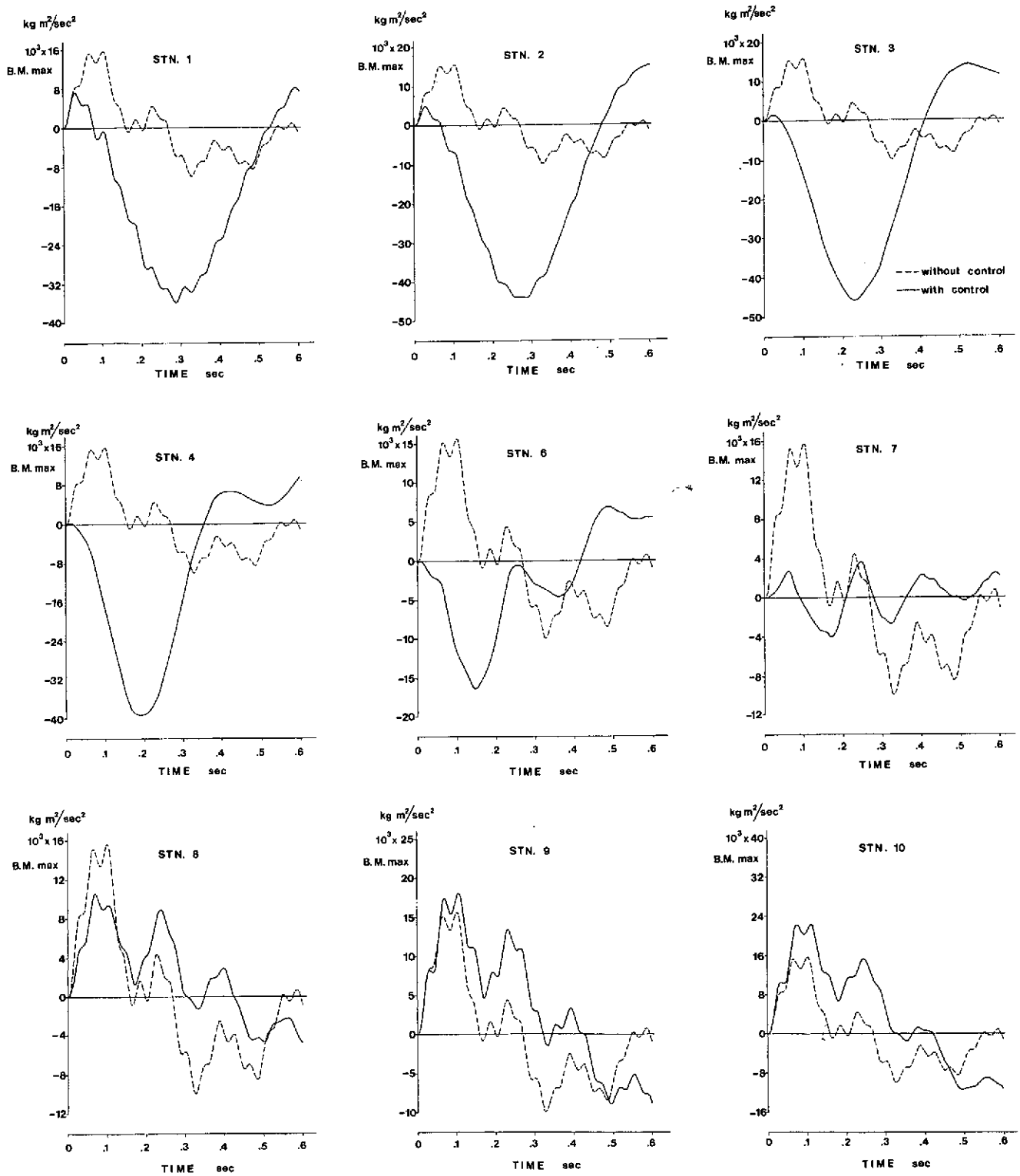

Figure 20: Variation with time of the maximum wing bending moment (at station 10) due to a step up gust - Westwind transport with a single L.E. - T. E. active system located at various stations along the wing.

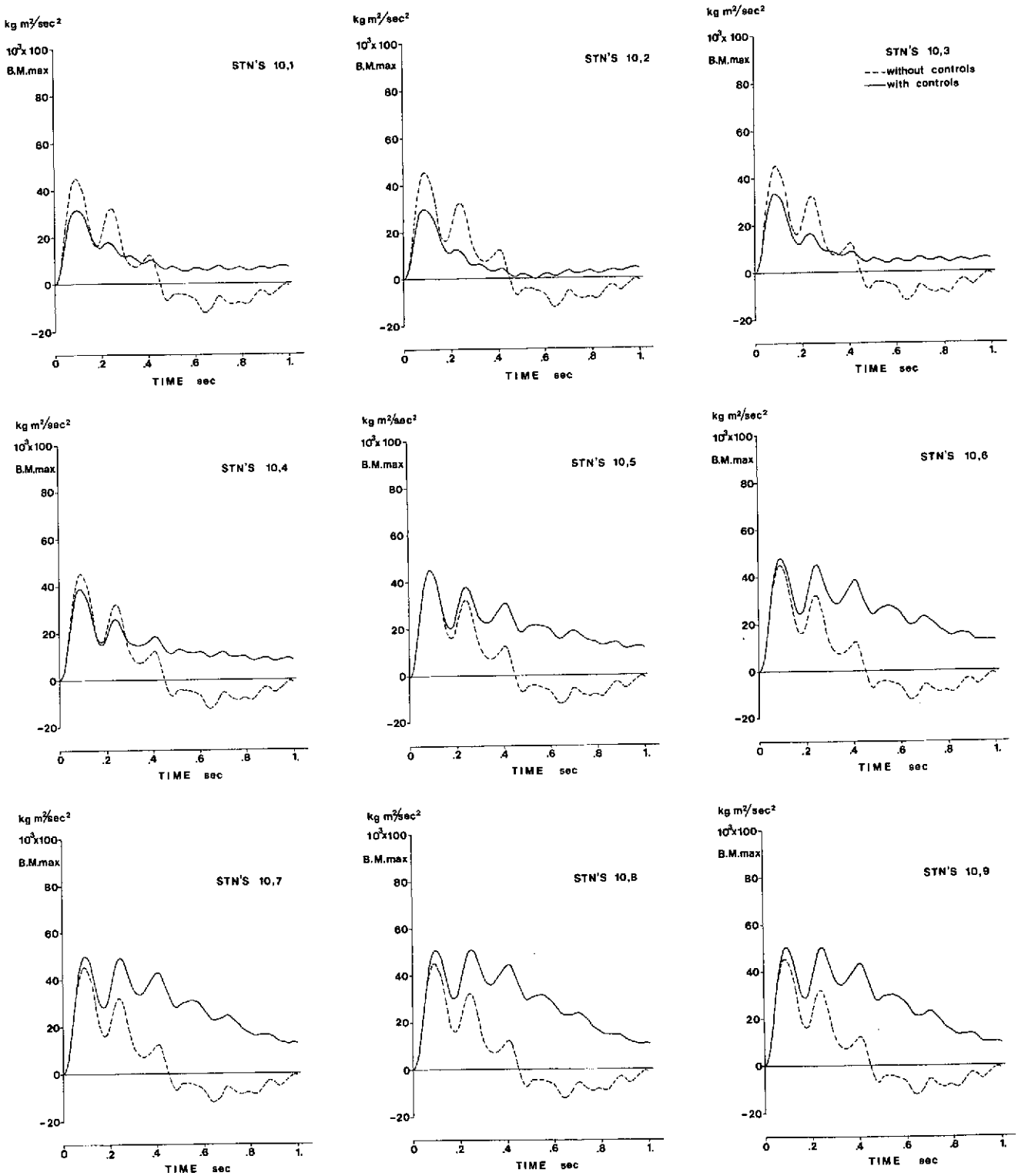

Figure 21: Variation with time of the maximum wing bending moment (at station 5) due to a step up gust - Arava transport with 2 L.E. - T.E. active systems: one located at station 10 and one located at various stations along the wing.

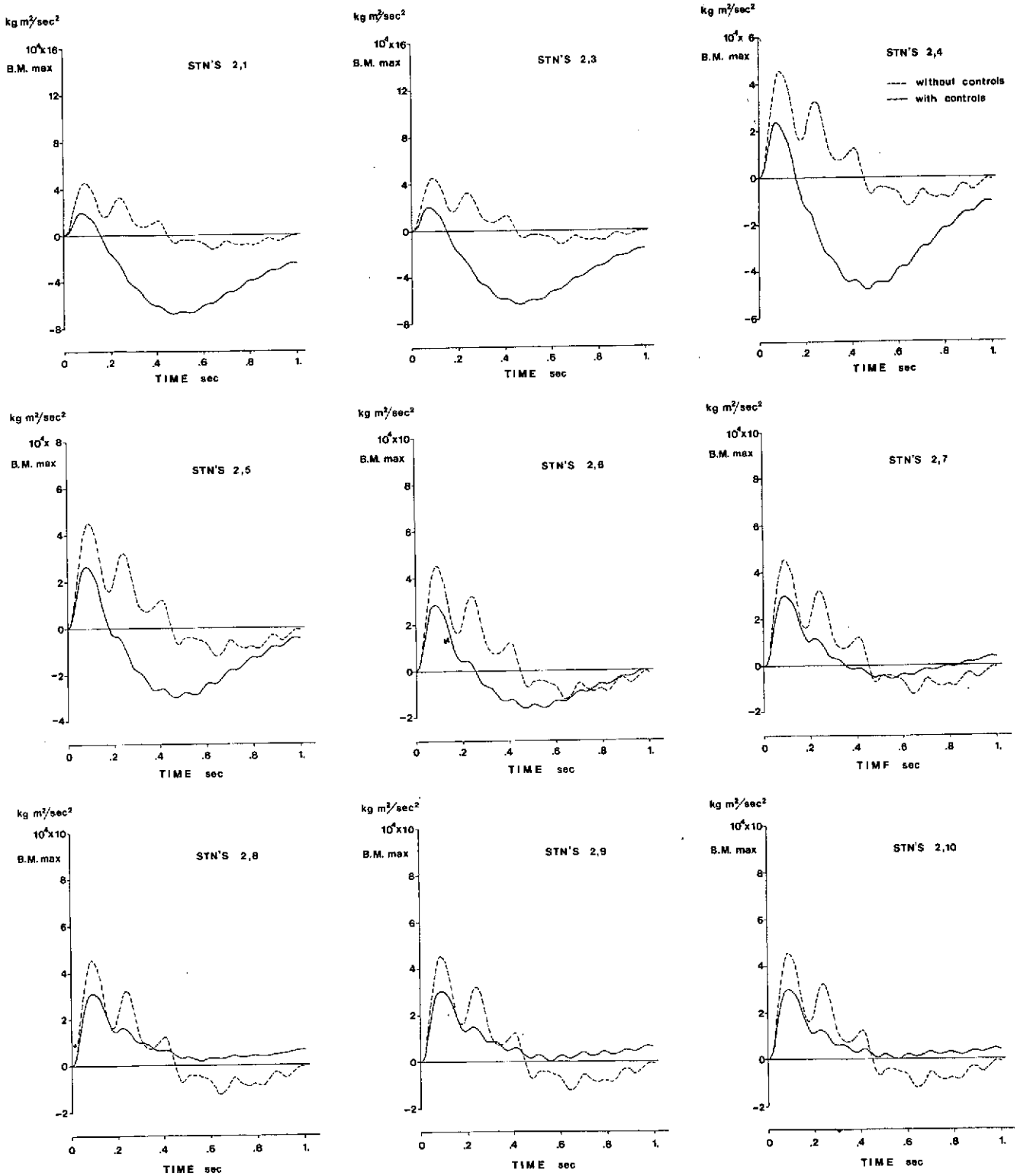

Figure 22: Variation with time of the maximum wing bending moment (at station 5) due to a step up gust - Arava transport with 2 L.E. - T.E. active systems: one located at station 2 and one located at various stations along the wing.

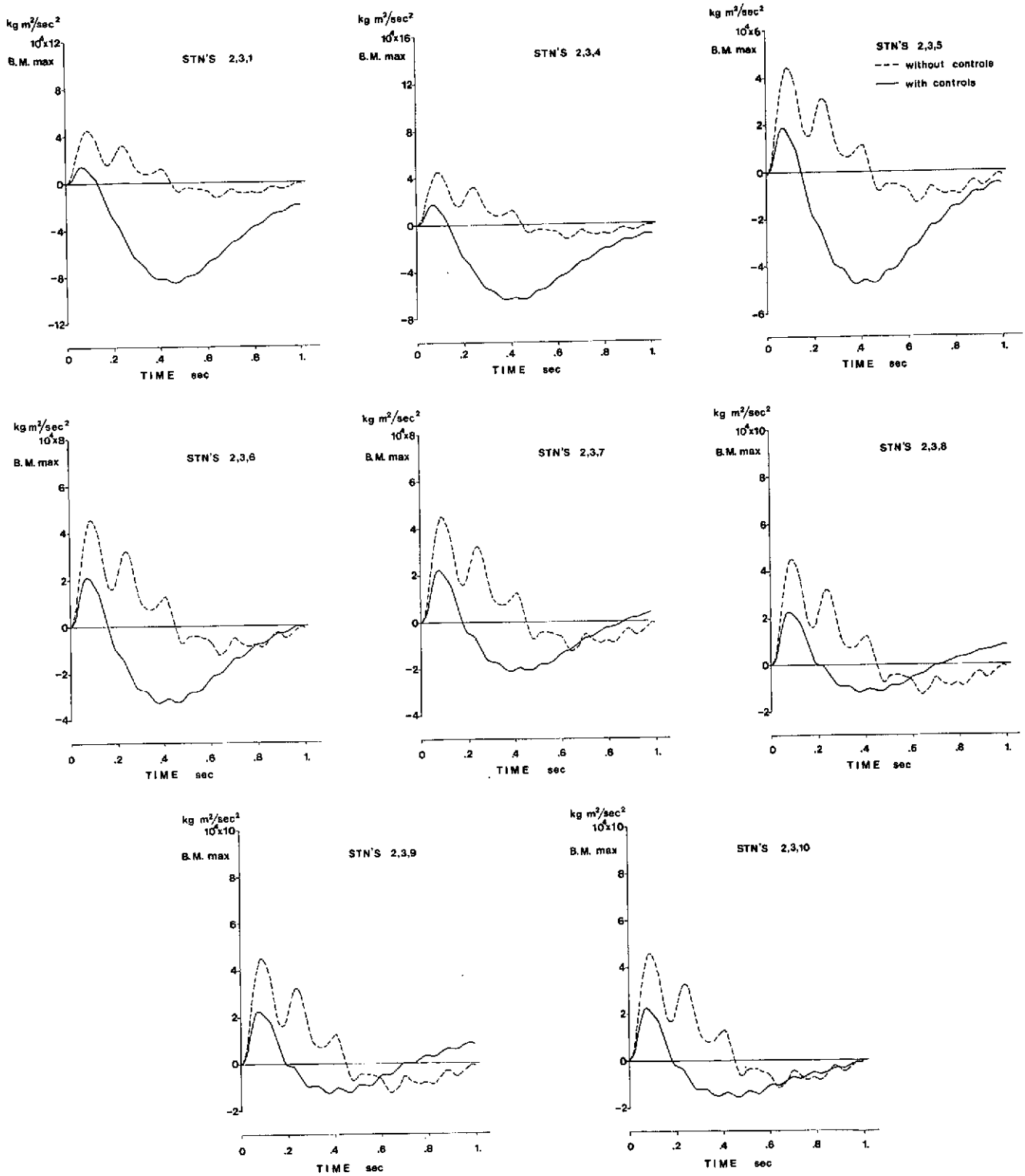

Figure 23: Variation with time of the maximum wing bending moment (at station 5) due to a step up gust - Arava transport with 3 L.E. - T.E. active systems: two located at stations 2 and 3 and one located at various stations along the wing.

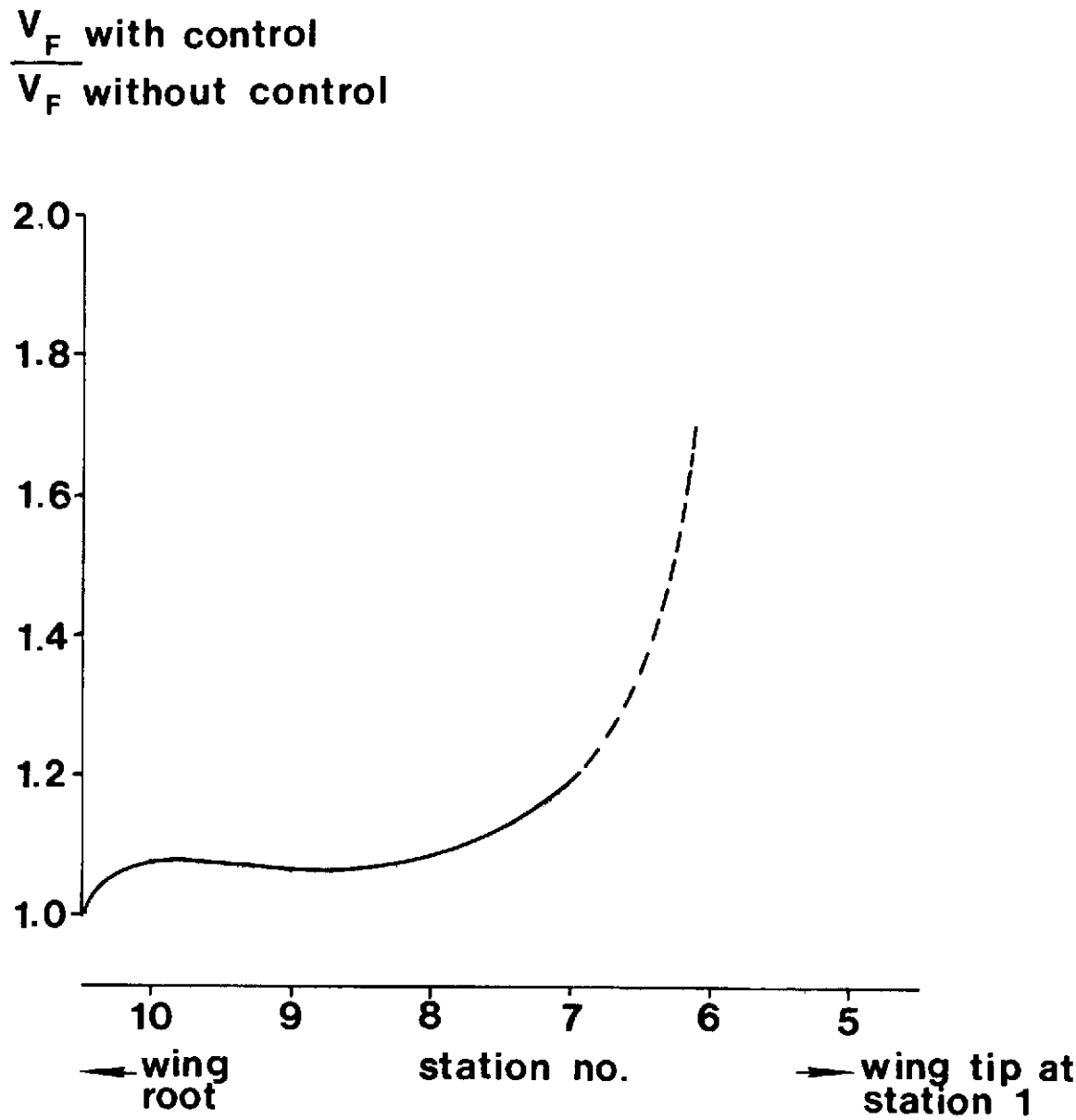

Figure 24: Variation of the flutter speed of the Arava transport with the location of a single L.E. - T.E. active system at the various stations along the wing.